early death in remission induction chemotherapy (death within 30 days) were 1 patient in Group A and 3 patients in Group B (Table 3). The cause of death in each group was infection or tumor progression. The completion rate of consolidation therapies were 37.3% in Group A (12 out of 33 evaluable cases), 37.9% in Group B (11 out of 29 evaluable cases). On the other hand, the maintenance therapies were completed 21.2% in Group A (7 out of 33 evaluable cases), and 15.2% in Group B (5 out of 33 evaluable cases). The numbers of dose attenuation in Group A were 30 patients of 100% dose, 21 patients of 80% or 60% dose and 2 patients of unknown.

Allogeneic hematopoietic stem cell transplantation (allo-HSCT) was performed in 11 out of 50 patients (22%) in Group A and 19 out of 66 patients (28.8%) in Group B. Among those who received allo-HSCT, the transplantation was performed during the first remission in 40%, 21% of patients in Groups A, B, respectively.

There were 15 patients who lived longer than 1,000 days after diagnosis: 6, 9 patients in Groups A, B, respectively. Regarding the transplantation among long-term survivors, 3 out of 6 patients were transplanted in Group A, 6 out of 9 in Group B. Comparing the achievement of CR among these patients in Groups A and B, all 6 patients in Group A achieved CR, but only 4 out of 9 patients in Group B achieved CR.

Table 3 Toxicity of the induction therapy

	A ($n = 53$) (range)	B ($n = 67$) (range)	P value (A vs. B)
Period of WBC <1,000 (day)	19 (0–44) $n = 49$	4 (0–50) $n = 63$	<0.0001
Toxicity (grade 3/4)			
Presence	19	13	0.427
Bleeding	2	1	ND
Infection	17	11	0.04
Others	2	2	ND
Early death (<30 days)	1	3	ND

Statistical analysis between Groups A and B was performed using the χ^2 test or Mann–Whitney U-test

ND not done

4 Discussion

In this MDS200 study, patients with high-risk MDS and AML transformed from MDS (MDS–AML) were treated with either intensive or low-dose remission induction therapy, followed by intensive post-remission therapy that was the same as in the JALSG MDS96 study [13].

Although we did not perform statistical comparison of DFS or OS between these two treatment groups due to the insufficient number of patients enrolled, the results suggest that there was no significant difference, that is, survival curves were superimposable (Figs. 2, 3). Intensive chemotherapy similar to that for AML can produce a CR rate of 64.7% for high-risk MDS and MDS–AML patients, whereas low-dose induction therapy can result in a CR rate of 43.9%. However, among the patients enrolled in this trial, the difference in CR rate did not lead to better survival as described above. In terms of adverse events, patients who received intensive treatment had more grade 3 or 4 adverse events, particularly infectious events with a longer period of leukopenia. There was no increase in the number of patients succumbing to early death (death within 30 days after the

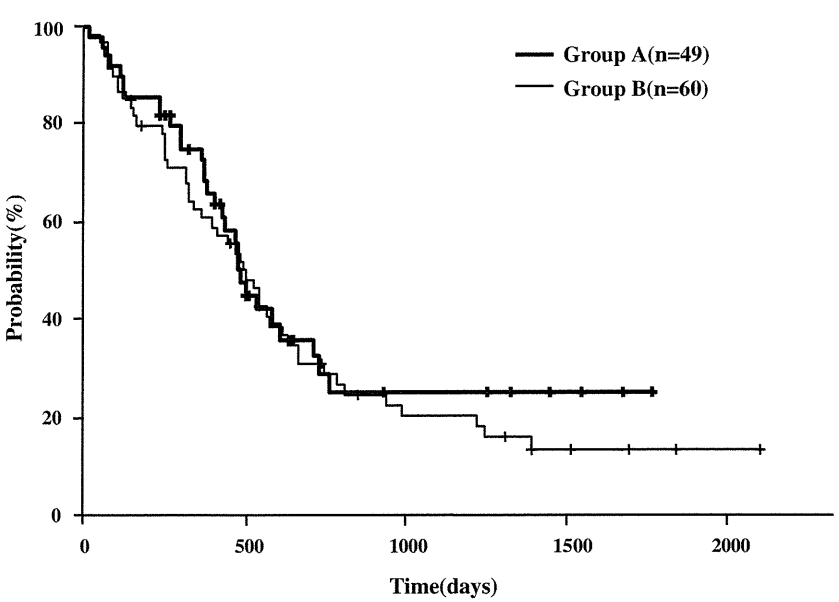

Fig. 2 Overall survival. Survival was calculated from the date of the start of treatment to the date of death due to any cause or to the date of the most recent follow-up. These data were not censored at the time of HSCT. All randomized patients were not included this data in each group. Due to this reason, some patients were not known to be CR or not, but known to be alive or not

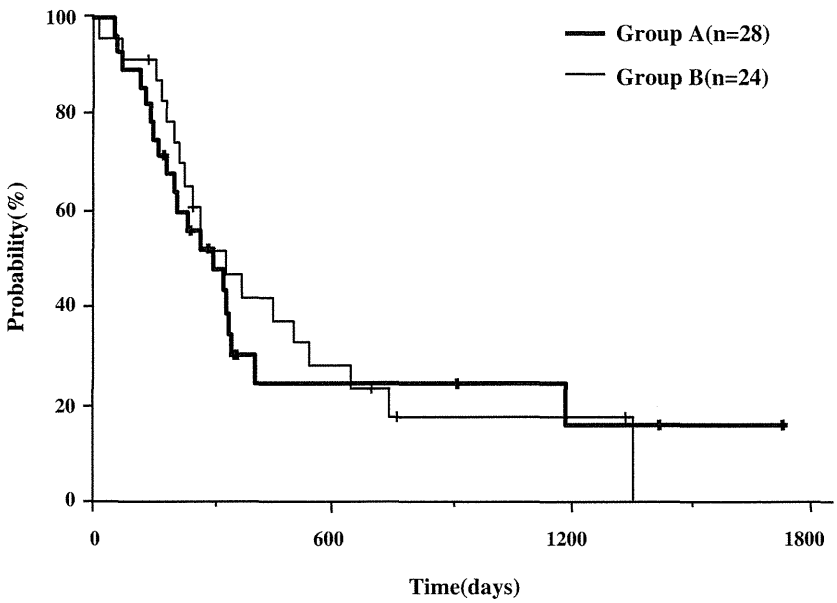

Fig. 3 Disease-/relapse-free survival. RFS was calculated from the date of achieving complete remission to the date of relapse, death or the most recent follow-up. These data were not censored at the time of HSCT. All randomized patients were not included this data in each group. Due to this reason, some patients were not known to be CR state or relapse, but known to be alive or not

start of treatment) in Group A, suggesting that intensive treatment produced higher CR rate, and higher toxicity resulted in a similar survival rate with low-dose induction therapy at least during the early phase of treatment.

There are several reasons that could explain why no difference in survival rate was observed regardless of the difference in CR rate. One could be the similar post-remission therapy between Groups A and B, as demonstrated by the almost similar DFS curves among the two groups. Another reason could be the disease status at the time of transplantation for patients in the two groups. In Group A, 60% of the transplantation was performed during the period other than that covering the first CR; this was 79% in Group B. Allo-HSCT has been shown to have the strongest antileukemia effect, and this was also found in the current study in which 6 out of 15 long-term survivors received allo-HSCT in Groups A and B. From the viewpoint of transplantation, intensive treatment merely selected cases that were suitable for transplantation, as observed in the case of transplantation for relapsed AML patients [17]. There are arguments against remission induction therapy for MDS patients in that it does not affect post-transplant prognosis [6, 18]. In the results of JSHCT, the chemotherapy before undergoing allo-SCT is not necessary in patients with MDS [6]. A group from the Institute of Medical Science of Tokyo University performed umbilical cord blood stem cell transplantation without remission induction therapy in high-risk MDS patients aged not more than 55 years and obtained favorable results with reduced time from diagnosis to transplantation [19]. It is important to perform clinical studies based on the concept that HCST should be performed immediately after diagnosis without remission induction, and determine the types of patients who would benefit from remission induction therapy prior to transplantation in terms of prognosis. In the present study, although suspended because of the insufficient number of patients enrolled, it appears that remission induction therapy with IDR and Ara-C did not produce better survival than that with low-dose chemotherapy despite higher CR rate. Therefore, it is suggested that CR rate is not a suitable surrogate marker for the evaluation of the outcome of chemotherapy for high-risk MDS and MDS–AML. In the latest reports, induction chemotherapy for patients with high-risk MDS and MDS–AML also provide no survival advantage [20, 21]. Considering the low survival rate of patients in this category, it is clearly necessary to introduce new strategies for the treatment of high-risk MDS and MDS–AML, such as molecular targeting agents and allo-HSCT with reduced-intensity conditioning regimens.

Acknowledgments We would like to thank the participating physicians in the Japan Adult Leukemia Study Group (JALSG) MDS200 study for their cooperation. This work was supported in part by grants-in-aid for Scientific Research from the Japanese Ministry of Education, Culture, Sport, Science, and Technology, and grants-in-aid for Cancer Research from the Japanese Ministry of Health, Labor, and Welfare.

References

1. Mhawech P. Myelodysplastic syndrome: review of the cytogenetic and molecular data. Crit Rev Oncol/Hematol. 2001;40:229–38.
2. Hofmann W, Koeffler HP. Myelodysplastic syndrome. Ann Rev Med. 2005;56:1–16.
3. Bennett JM, Catovsky D, Daniel MT, Flandrin G, Galton DA, Gralnick HR, et al. Proposals for the classification of the myelodysplastic syndromes. Br J Haematol. 1982;51:189–99.

4. Finke J, Nagler A. Viewpoint: what is the role of allogeneic haematopoietic cell transplantation in the era of reduced-intensity conditioning—is there still an upper age limit? A focus on myeloid neoplasia. Leukemia. 2007;21:1357–62.
5. Tricot GJ. Prognostic factors in myelodysplastic syndrome. Leuk Res. 1992;16:109–15.
6. Nakai K, Kanda Y, Fukuhara S, Sakamaki H, Okamoto S, Kodera Y, et al. Value of chemotherapy before allogeneic hematopoietic stem cell transplantation from an HLA-identical sibling donor for myelodysplastic syndrome. Leukemia. 2005;19:396–401.
7. De Witte T. Stem cell transplantation for patients with myelodysplastic syndrome and secondary leukemias. Int J Hematol. 2000;72:151–6.
8. Cutler CS, Lee SJ, Greenberg P, Deeg HJ, Perez WS, Anasetti C, et al. A decision analysis of allogeneic bone marrow transplantation for the myelodysplastic syndrome: delayed transplantation for low risk myelodysplasia is associated with improved outcome. Blood. 2004;104:579–85.
9. Oran B, Giralt S, Saliba R, Hosing C, Popat U, Khouri I, et al. Allogeneic hematopoietic stem cell transplantation for the treatment of high-risk acute myelogenous leukemia and myelodysplastic syndrome using reduced-intensity conditioning with fludarabine and melphalan. Biol Blood Marrow Transplant. 2007;13:454–62.
10. Lekakis L, de Lima M. Reduced-intensity conditioning and allogeneic hematopoietic stem cell transplantation for acute myeloid leukemia. Expert Rev Anticancer Ther. 2008;8:785–98.
11. Denzlinger C, Bowen D, Benz D, Gelly K, Brugger W, Kanz L. Low-dose melphalan induces favourable responses in elderly patients with high-risk myelodysplastic syndromes or secondary acute leukaemia. Br J Haematol. 2000;108:93–5.
12. Miller KB, Kim K, Morrison FS, Winter JN, Bennett JM, Neiman RS, et al. The evaluation of low-dose cytarabine in the treatment of myelodysplastic syndrome. Ann Hematol. 1992;65:162–8.
13. Okamoto T, Kanamaru A, Shimazaki C, Motoji T, Takemoto Y, Takahashi M, et al. Combination chemotherapy with risk factor-adjusted dose attenuation for high-risk myelodysplastic syndrome and resulting leukemia in the multicenter study of the Japan Adult Leukemia Study Group (JALSG): results of an interim analysis. Int J Hematol. 2000;72:200–5.
14. Greenberg P, Cox C, LeBeau MM, Fenaux C, Morel P, Sanz G, et al. International scoring system for evaluating progenitors in myelodysplastic syndrome. Blood. 1997;89:2079–88.
15. Yamada K, Furusawa S, Saito K, Waga K, Koike T, Arimura H, et al. Concurrent use of granulocyte colony-stimulating factor with low-dose cytosine arabinoside and aclarubicin for previously treated acute myelogenous leukemia: a pilot study. Leukemia. 1995;9:10–4.
16. Miller AB, Hoogstraten B, Staquet M, Winkler A. Reporting results of cancer treatment. Cancer. 1981;47:207–14.
17. Alessandrino EP, Della Porta MG, Bacigalupo A, Van Lint MT, Falda M, Onida F, et al. WHO classification and WPSS predict post-transplantation outcome in patients with myelodysplastic syndrome: a study from the Gruppo Italiano Trapianto di Midollo Osseo (GITMO). Blood. 2008;112:895–902.
18. Nachtkamp K, Kundgen A, Strupp C, Giagounidis A, Kobbe G, Gattermann N, et al. Impact on survival of different treatments for myelodysplastic syndromes (MDS). Leuk Res. 2009;33:1024–8.
19. Ooi J. The efficacy of unrelated cord blood transplantation for adult myelodysplastic syndrome. Leuk Lymphoma. 2006; 47:599–602.
20. Knipp S, Hildebrand B, Kundgen A, Giagounidis A, Kobbe G, Haas R, et al. Intensive chemotherapy is not recommended for patients aged >60 years who have myelodysplastic syndromes or acute myeloid leukemia with high-risk karyotypes. Cancer. 2007;110:345–51.
21. Fenaux P, Mufti GJ, Hellstrom-Lindberg E, Santini V, Finelli C, Giagounidis A, et al. Efficacy of azacitidine compared with that of conventional care regimens in the treatment of higher-risk myelodysplastic syndromes: a randomized, open-rabell, phase III study. Lancet Oncol. 2009;10:223–32.

Ann Hematol (2010) 89:1255–1263
DOI 10.1007/s00277-010-1020-3

ORIGINAL ARTICLE

Autoantibodies specific to hnRNP K: a new diagnostic marker for immune pathophysiology in aplastic anemia

Zhirong Qi · Hiroyuki Takamatsu · J. Luis Espinoza · Xuzhang Lu · Naomi Sugimori · Hirohito Yamazaki · Katsuya Okawa · Shinji Nakao

Received: 2 February 2010 / Accepted: 16 June 2010 / Published online: 10 July 2010

Abstract To identify a new diagnostic marker for the immune pathophysiology of aplastic anemia (AA), we screened sera of immune-mediated AA patients for the presence of antibodies (Abs) specific to proteins derived from a leukemia cell line UT-7 using two-dimensional electrophoresis followed by immunoblotting. The target proteins were identified by peptide mass fingerprinting. Heterogeneous nuclear ribonucleoprotein (hnRNP) K was identified as a novel autoantigen. An enzyme-linked immunosorbent assay revealed high titers of anti-hnRNP K Abs in 85 (31%) of 273 patients with AA. Sixty-four patients received antithymocyte globulin and cyclosporine after undergoing screening for anti-hnRNP K Ab, anti-DRS-1 Ab, anti-moesin Ab, and paroxysmal nocturnal hemoglobinuria (PNH)-type cells. Twenty (87%) of 23 patients with the presence of anti-hnRNP K Abs responded to the immunosuppressive therapy (IST), while 19 (46%) of 41 patients without the presence of anti-hnRNP K Abs responded. A multivariate analysis showed only PNH-type cells and anti-hnRNP K Abs to be significant factors for the prediction of a good response to IST. The detection of anti-hnRNP K Abs as well as PNH-type cells may therefore be useful for diagnosing the immune pathophysiology of AA.

Keywords Aplastic anemia · hnRNP K · Autoantibody · Bone marrow failure

Z. Qi · H. Takamatsu · J. L. Espinoza · X. Lu · N. Sugimori · H. Yamazaki · S. Nakao (✉)
Cellular Transplantation Biology, Kanazawa University Graduate School of Medical Science,
13-1 Takaramachi,
Kanazawa 920-8641, Japan
e-mail: snakao@med3.m.kanazawa-u.ac.jp

Z. Qi
West China Medical Center, Sichuan University,
Chengdu, China

K. Okawa
Biomolecular Characterization Unit, Frontier Technology Center,
Kyoto University Graduate School of Medicine,
Kyoto, Japan

Introduction

A large amount of laboratory and clinical data including a good response to immunosuppressive therapy (IST) suggest that the immune system attack against hematopoietic stem cells plays an essential role in the pathophysiology of aplastic anemia (AA). More than 70% of all patients with AA respond to IST with antithymocyte globulin (ATG) and cyclosporine (CsA) [1, 2]. However, IST may be detrimental to patients with non-immune-mediated AA because it potentially increases the risk of opportunistic infections and delays treatment with allogeneic stem cell transplantation. Several markers predicting good response to IST in patients with AA have been proposed. These include an increased ratio of activated T cells [3], increased interferon-γ expression in bone marrow (BM) and peripheral blood T cells [4, 5], increased expression of heat shock protein 72 [6], the presence of HLA-DRB1*1501, and small population of paroxysmal nocturnal hemoglobinuria (PNH)-type cells [7, 8]. Recent studies have demonstrated the presence of PNH-type cells to be the most reliable predictor of good response to IST [9]. However, the method for detecting small populations of PNH-type cells has not yet been generalized, possibly due to inter-lab differences in the sensitivity and the specificity of flow cytometry. PNH-type cells cannot be utilized to diagnose immune pathophysiology when fresh blood containing a sufficient number of granulocytes from patients is unavailable. Furthermore,

approximately 48% of AA patients not bearing small populations of PNH-type cells (PNH^- patients) respond to ATG and CsA therapy [8]. More reliable and universal assays that supplement the role of PNH-type cell detection are therefore required to predict a good response to IST in patients with AA.

Autoimmune diseases such as multiple sclerosis (MS) and insulin-dependent diabetes mellitus (IDDM) are characterized by the presence of autoantibodies (auto-Abs) specific to antigens derived from target organs, such as myelin basic protein in MS and glutamate decarboxylase in IDDM. These autoantibodies are detectable in the patients' sera, and the Abs serve as a marker of the immune pathophysiology of these diseases [10, 11]. Two auto-Abs specific to diazepam-binding inhibitor-related protein-1 (DRS-1) and moesin were recently identified in the sera of patients with AA. These Abs were detectable in 38% and 37% of AA patients bearing increased PNH-type cells (PNH^+ patients), but the prevalence of the Abs in PNH^- patients with AA was only 6% and 21%, respectively [12, 13]. Therefore, these Abs do not help in the diagnosis of the immune pathophysiology in PNH^- patients with AA. The identification of novel auto-Abs is therefore needed to improve the accuracy of predicting good response to IST.

This study screened sera from patients with PNH^+ AA for the presence of Abs recognizing antigens derived from a megakaryocytic leukemia cell line UT-7 using two-dimensional electrophoresis (2-DE) followed by immunoblotting and peptide mass fingerprinting.

Materials and methods

Sera and cell lines

Sera were obtained from 273 Japanese patients with AA at the time of the diagnosis. Table 1 shows characteristics of patients with AA. AA was diagnosed at Kanazawa University hospital and other hospitals taking part in the bone marrow failure (BMF) study group led by the Ministry of Health, Labor, and Welfare of Japan from December 2007 to March 2009. Sera were also obtained from 33 Japanese patients with rheumatoid arthritis (RA). Sera from 96 healthy individuals were used as controls. Samples were cryopreserved at −80°C until use. UT-7 was kindly provided by Dr N. Komatsu of Jichi Medical School. OUN-1, a cell line derived from chronic myelogenous leukemia, was kindly provided by Dr M. Yasukawa of the Ehime University. K562 and HL-60 cell lines were purchased from the Health Science Research Resource Bank (Osaka, Japan). All patients and healthy individuals provided their informed consent in accordance with the Declaration of Helsinki before sampling. This study was approved by the human research ethical committee of Kanazawa University Graduate School of Medical Science.

Table 1 Patient characteristics

Characteristics	Number	Range
Total (*n*)	273	NA
Age at diagnosis (year)	52.7	14–91
Gender (male/female)	141/132	NA
Severity (severe/moderate)	118/155	NA
Neutrophil count ($\times 10^9$/L)	830	0–2,325
Platelet count ($\times 10^9$/L)	22	2–126
Reticulocyte count ($\times 10^9$/L)	29	2–114

NA not applicable

Detection of PNH-type cells

Peripheral blood was subjected to high-sensitivity two-color flow cytometry to detect small populations of glycosylphosphatidylinositol-anchored membrane protein-deficient cells in granulocytes and erythrocytes, as described previously [8]. The presence of ≥0.003% $CD55^-CD59^-CD11b^+$ granulocytes and ≥0.005% $CD55^-CD59^-$glycophorin-A^+ erythrocytes was defined as an abnormal increase based on the results of 183 healthy individuals [9].

2-DE and western blotting

2-DE was performed as described previously with some modifications [14]. A total of 10^6 UT-7 cells were solubilized with sample preparation solution containing 7 M urea, 2 M thiourea, 4% CHAPS, 2% immobilized pH gradients (IPG) buffer pH 3–10, and 40 mM dithiothreitol (DTT; GE Healthcare, Tokyo, Japan), and the sample was diluted to 125 μl with thiourea rehydration buffer containing 7 M urea, 2 M thiourea, 2% IPG-buffer pH 3–10, 0.002% bromophenol blue, and 2.8 mg/ml DTT. Before loading into IPG-strips, the diluted sample was cleared by centrifugation (13,000 rpm for 20 min), applied to 7-cm non-linear Immobiline DryStrip of pH 3–10 (GE Healthcare) and incubated for 12 h at room temperature; then the IPG strip was subjected to first-dimensional isoelectric focusing electrophoresis (IFE) using the flatbed multiphor II electrophoresis system (GE Healthcare). The IPG strip after IFE was equilibrated twice at room temperature for 10 min with 10 ml of SDS equilibration buffer solution (6 M urea, 75 mM Tris–HCl pH 8.8, 29.3% glycerol, 2% SDS, 0.002% bromophenol blue, and 100 mg DTT or 250 mg iodoacetamide) and subjected to second dimensional SDS-PAGE. Separated proteins were transferred onto a polyvinylidene fluoride (PVDF) membrane (Millipore

Corporation, Bedford, USA) for 1.5 h at a constant current of 190 mA using a Mini Trans-Blot system (Bio-Rad, Hercules, CA) or visualized by Coomassie Brilliant Blue (CBB) staining. The blotted PVDF membranes were incubated in the presence of Tris-buffered saline (TBS) with 1% bovine serum albumin (BSA) containing serum diluted 1:200 from the patients, serum diluted 1:200 from healthy individuals or 1:2,000 diluted mouse anti-human heterogeneous nuclear ribonucleoprotein (hnRNP) K/J monoclonal Ab (mAb, clone 3C2, Sigma, USA), and then were reacted with appropriate alkaline phosphatase-labeled secondary Abs and the immunoblots were detected using a BCIP/NBT membrane alkaline phosphatase substrate system (KPL, Gaithersburg, MD, USA).

Isolation of $CD34^+$ cell

$CD34^+$ cells were isolated from the BM of healthy volunteers using a CD34 progenitor cell isolation kit (Miltenyi Biotec, Bergisch Gladbach, Germany) according to the manufacturer's instructions.

Protein identification

The proteins recognized by serum Abs were identified as previously describe [15, 16]. Briefly, after SDS-PAGE, proteins were visualized by CBB staining, and the pieces of the gel corresponding to western blotting-positive spots were excised, followed by in-gel digestions with trypsin. Molecular mass analyses of tryptic peptides were performed by matrix-assisted laser desorption/ionization time of flight mass spectrometry (MALDI-TOF MS) using an ultraflex TOF/TOF system.

Construction of the recombinant plasmid and purification of bacterially expressed protein

Full-length hnRNP K cDNA kindly provided by H. Sorimachi (Tokyo Metropolitan Organization for Medical Research) was subcloned into the pGEX-6p-1 vector (GE Healthcare) for the expression of glutathione-*S*-transferase (GST) fusion protein. Synthesized proteins were purified by glutathione sepharose 4B (GE Healthcare) according to the manufacturer's instructions. Native hnRNP K proteins were released from GST-hnRNP K fusion proteins using PreScission protease (GE Healthcare). The recombinant protein was confirmed by CBB staining and western blotting with anti-hnRNP K/J mAb.

Immunoprecipitation

Immunoprecipitation detection of anti-hnRNP K Abs using sera from patients with AA was performed according to the instructions of the Seize X Protein G Immunoprecipitation Kit (Pierce, Illinois, USA). Briefly, 10 μl of serum samples were incubated for 2 h at 4°C with 400 μl protein G-agarose beads (Pierce), and then the beads were washed three times with binding/wash buffer with centrifugation (10,000×*g* for 3 min). The beads were incubated in 200 μl of binding/wash buffer containing 1 μg of purified native hnRNP K protein for overnight at 4°C; then the beads were pelleted by centrifugation (10,000×*g* for 3 min). Thereafter, they were washed five times before the proteins were eluted from the beads with 50 μl of elution buffer for SDS-PAGE and western blotting with anti-hnRNP K/J mAb.

Determination of hnRNP K expression by hematopoietic cells

Lysates of myeloid leukemia cell lines, $CD34^+$, and peripheral blood mononuclear cells (PBMCs) from healthy individuals were obtained by suspending cell pellets in 100 μl of phosphate-buffered saline (PBS) containing protease inhibitor cocktail (Sigma Aldrich), sonicated on ice for 20 s using a B-12 Branson sonifier (Danbury, CT, USA). The cell lysates were then denatured in boiling SDS sample buffer. Equal amounts of proteins were separated by SDS-PAGE and transferred onto PVDF membrane. The membrane was incubated in 1% BSA–TBS containing 1:2,000 diluted anti-hnRNP K/J mAb or 1:5,000 diluted mouse anti-human α-tubulin mAb (clone B-5-1-2, Sigma, USA), respectively.

Enzyme-linked immunosorbent assay

Fifty microliters of coating buffer (50 mM carbonate/bicarbonate buffer, pH 9.6) containing 1 μg/ml recombinant native hnRNP K protein, recombinant native DRS-1 protein, or recombinant native moesin protein was added to each well of a 96-well Nunc-Immuno plate (Nalge-Nunc International, Roskilde, Denmark) and kept overnight at 4°C. The plates were washed and incubated with PBS containing 10% fetal bovine serum for 2 h at 37°C to block nonspecific binding. The sera from patients were added to a final dilution of 1:200 at room temperature for 2 h. After washing, the plates were incubated with 100 μl of peroxidase-conjugated goat anti-human IgG Ab (1:100,000; Jackson ImmunoResearch) at room temperature for 1 h. Finally, plates were washed and incubated with 3,3,5,5-tetramethylbenzidine substrate (Pierce, Rockford, IL) at room temperature for 30 min, and the optic density (OD) absorbance at 450 nm was read using a SLTEAR 340 ATELISA reader (SLT-Labinstruments, Grödig, Austria). A positive reaction (Ab^+) was defined as an absorbance value exceeding the mean+2 standard deviation (SD) of the OD absorbance values from the sera of the 96 healthy individuals.

Immunosuppressive therapy

Sixty-four patients with AA were treated with ATG (Lymphoglobuline, Aventis Behring, King of Prussia, PA) 15 mg/kg/day, 5 days, plus CsA (Novartis, Basel, Switzerland) 6 mg/kg/day within 1 year of diagnosis between December 2007 and March 2009. The dose of CsA was adjusted to maintain trough levels between 150 and 250 ng/ml, and the appropriate dose was administered for at least 6 months. Granulocyte colony-stimulating factor (G-CSF; filgrastim, 300 μg/m^2 or lenograstim, 5 μg/kg) was administered to some patients. The response to IST was assessed at 6 months after the IST according to the criteria proposed by Camitta [17].

Statistics

Differences in the prevalence of hnRNP K Abs among different groups were examined using a one-way analysis of variance. Correlations of anti-hnRNP K Ab titers with anti-moesin Ab titers or anti-DRS-1 Ab titers in individual patients were examined using student *t* test. The prevalence of anti-hnRNP K Abs between untransfused and transfused patients and the response rate to IST between Ab$^+$ and Ab$^-$ patients were examined using the Fisher's exact test. Logistic procedures and Fisher's exact test were used to analyze the associations between the response to IST and the prevalence of increased PNH-type cells, gender, age, severity, or three different Abs.

Results

Detection of novel auto-Abs in AA patients' sera

To detect auto-Abs specific to proteins derived from UT-7 cells, cell lysates were separated by 2-DE and subjected to western blotting using sera obtained from two PNH$^+$ untransfused patients with AA at the time of diagnosis. The sera from two patients revealed the same spot with a size of 65 kDa (Fig. 1a—ii) which was not seen on the membrane incubated with healthy individual sera (Fig. 1a—iii). The approximate isoelectric point was between 5 and 6.

Identification of the 65-kDa protein

The stained spot corresponding to the one showing positive reaction in the western blotting (Fig. 1a–i) was excised from the CBB stained gel. The proteins were eluted from the excised gel after in-gel enzyme digestion and were subjected to MALDI-TOF MS. The protein was identified as hnRNP K of which isoelectric point is 5.46. Anti-hnRNP K/J mAb revealed the same spot identified by the incubation with the patient sera (Fig. 1a—iv). Specific binding of the patients' anti-hnRNP K Abs to hnRNP K was confirmed by an immunoprecipitation analysis (Fig. 1b).

Expression of hnRNP K by hematopoietic cells

The level of expression of hnRNP K was greater in several myeloid leukemia cell lines such as HL-60, OUN-1, UT-7, and K562 than in PBMCs from healthy individuals, but there was no difference in the hnRNP K expression level between CD34$^+$ cells and PBMCs from healthy individuals (Fig. 2).

Prevalence of anti-hnRNP K Abs in patients with AA and RA

The titers of Ab specific to hnRNP K in the sera of 273 AA and 33 RA patients were determined using enzyme-linked immunosorbent assay (ELISA) with the recombinant human native hnRNP K proteins (Fig. 3a). The titers of Ab specific to hnRNP K in the sera of 273 AA and 33 RA patients were determined using ELISA with the recombinant human native hnRNP K proteins (Fig. 3a). High titers of anti-hnRNP K Abs (≥ the mean±2SD of the titers of healthy individuals, anti-hnRNP K Ab$^\pm$) were detected in 85 (31%) of the AA patients and in eight (24%) of the RA patients. There was no significant difference in the prevalence of anti-hnRNP K Abs between AA and RA patients ($P \geq 0.05$). There was no difference in the prevalence of anti-hnRNP K Abs between untransfused (27%) and transfused (33%) AA patients ($P = 0.33$). Small populations of PNH-type cells were detectable in 155 (56%) of the AA patients, and the prevalence of anti-hnRNP K Abs in PNH$^+$ and PNH$^-$ AA patients was 36% and 25%, respectively.

Correlation of anti-hnRNP K Abs with other auto-Abs

Anti-hnRNP K Ab with anti-DRS-1 Ab or anti-moesin Ab titers were measured from the same patients' sera to determine the relationship between these Abs. The anti-DRS-1 Abs and anti-moesin Abs were detectable in 29% and 28% of the 273 patients with AA, respectively. The titers of anti-hnRNP K Abs positively correlated with the presence of anti-DRS-1 Abs ($r = 0.5838$) and anti-moesin Abs ($r = 0.7239$; $P < 0.0001$; Fig. 3b).

Correlation of anti-hnRNP K Abs with response to IST

Sixty-four patients with AA of the 273 patients received ATG plus CsA therapy after the screening of three different

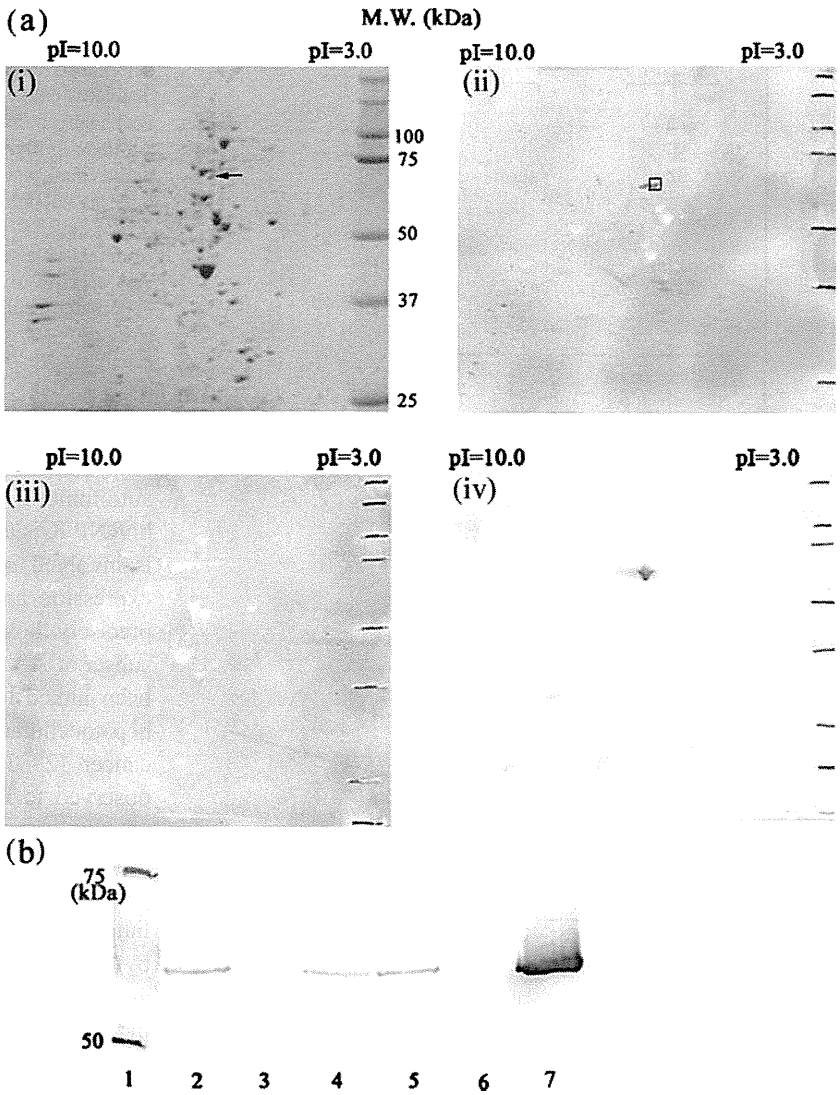

Fig. 1 Identification of the proteins derived from UT-7 cells recognized by serum Abs. **a** hnRNP K auto-Ab in serum from patient with AA. *i* UT-7 cell lysates were separated by 2-DE and visualized by CBB staining. The protein spot indicated by the *arrow* was identified as hnRNP K by mass spectrometry. *ii* UT-7 cell lysates were separated by 2-DE, transferred onto PVDF membrane, and then incubated with diluted AA patient serum (1:200). *iii* PVDF membrane was incubated with diluted healthy individual serum (1:200). *iv* PVDF membrane was incubated with diluted anti-hnRNP K/J mAb (1:2,000). **b** Immunoprecipitation detection of anti-hnRNP K Ab in the sera of patients with BMF. An equal amount of purified native hnRNP K proteins was incubated in the serum from AA patients (*lanes 2*, *4*, and *5*) and healthy individuals' sera (*lanes 3* and *6*). Anti-hnRNP K/J mAb at a 1:2,000 dilution was used as a positive control (*lane 7*)

Abs and PNH-type cells. Twenty (87%) of 23 patients with anti-hnRNP K Ab^+ responded to the IST, while 19 (46%) of 41 patients with anti-hnRNP K Ab^- responded (P=0.0015, Fig. 4a). When anti-hnRNP K Ab^+ patients were divided into two groups according to the Ab titers, there was no difference in the response rate to IST between very high titer (≥0.4, 93%) and moderately high titer (<0.4, 87%) groups (P=1.00). The response rate to IST in patients with at least one Ab^+ of three auto-Abs including anti-hnRNP K Ab, anti-DRS-1 Ab, and anti-moesin Ab was 81%, while the response rate in patients not showing Ab^+ in any of the three auto-Abs was 42% (P=0.0022; Fig. 4b). In 32 patients not displaying PNH-type cells, the response rate to IST with anti-hnRNP K Ab^+ was 86%, while only 32% patients with anti-hnRNP K Ab^- responded (P=0.0265; Fig. 4c). Multivariate analysis showed the presence of anti-hnRNP K Abs and PNH-type cells to be significant factors in the prediction of good response to IST (Table 2). Anti-hnRNP K Ab titers could be serially determined for 13 patients before and 6–7 months after IST. Four of the 13 patients showed high anti-hnRNP K Ab titers before IST. The Abs titers did not decrease either in three patients (pre-IST/post-IST: 0.3625/0.3635, 0.513/1.2455, 0.2875/0.2932) responding to IST or in one patient refractory to IST (0.413/0.318).

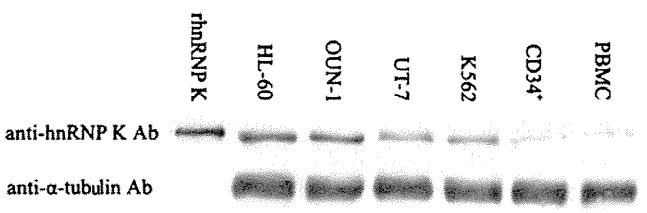

Fig. 2 Expression of hnRNP K by immature hematopoietic cells and PBMCs. An equal amount (20 μg) of cell extracts or recombinant hnRNP K protein was separated by 8% SDS-PAGE, transferred to PVDF membrane, and reacted with anti-hnRNP K/J mAb at a 1:2,000 dilution or anti-α-tubulin mAb at a 1:5,000 dilution

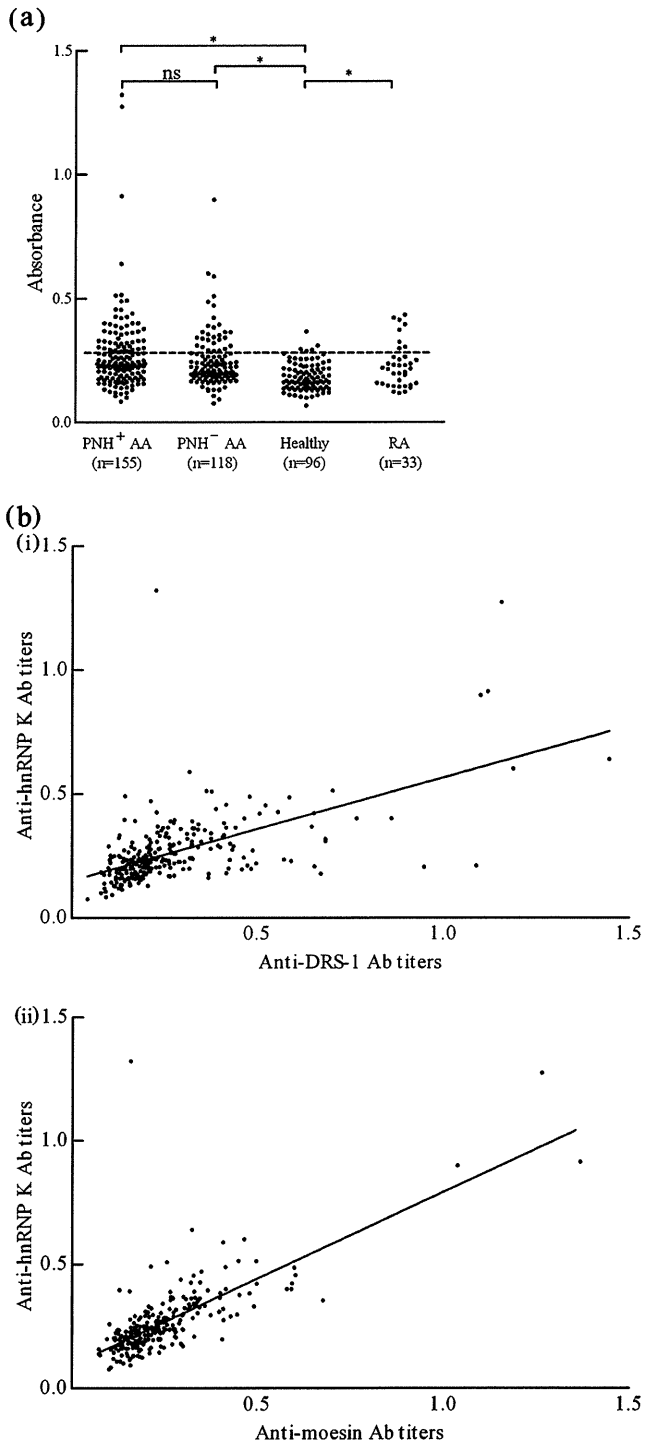

◀ **Fig. 3** Titration of anti-hnRNP K Abs in patients' sera using ELISA. **a** Antibody titers against purified hnRNP K proteins in the sera were determined using diluted sera at a 1:200 dilution. The *dotted line* denoted a cutoff value defined as the mean+2SD of the absorbance in 96 healthy individuals. *Asterisks* indicate a prevalence of hnRNP K Ab titers in PNH^+ AA, PNH^- AA, and RA patients' sera significantly higher than that of hnRNP K Ab titers in healthy individuals (*$P<0.05$; *ns* no significant meaning). **b** The correlation between the titers of anti-hnRNP K Ab and either anti-DRS-1 Ab or anti-moesin Ab from the same sera obtained from AA patients was examined. Titers of Abs specific to native hnRNP K, DRS-1, and moesin protein were determined using diluted sera at a 1:200 dilution, and correlations of anti-hnRNP K Ab titers with each of other two Ab titers (*i* and *ii*) were calculated ($P<0.0001$)

Discussion

The present study identified anti-hnRNP K Abs as a novel auto-Ab in the serum of patients with immune-mediated AA. hnRNPs are among the most abundant proteins in the eukaryotic cell nucleus and play a direct role in several aspects of RNA activity including splicing, export of the mature RNAs, and translation. Approximately 30 hnRNPs have been identified [18]. More and more evidence points to hnRNPs as important intracellular target antigens of the autoimmune response in autoimmune diseases [19–25]. hnRNP K is a conserved RNA/DNA-binding protein which is involved in the multiple steps that comprise both gene expression and signal transduction [26, 27]. It is unclear precisely how the anti-hnRNP K Abs were raised in a subset of AA patients. The overexpression of hnRNP K has been linked to a range of cancers including breast cancer, hepatocellular carcinoma, esophageal cancer, and colorectal cancer [28–31]. The hnRNP K protein expression was observed to increase in the $CD34^+$ bone marrow cells of patients with CML in the accelerated and blastic phase, but it did not increase in the $CD34^+$ cells of chronic phase CML patients and of healthy donors [32]. The present study failed to detect an increased expression of hnRNP K protein by $CD34^+$ cells from healthy individuals as well. However, an increased expression of hnRNP K was detectable in all of the examined myeloid leukemia cell lines. It is therefore possible that the destruction of immature hematopoietic cells that express high levels of hnRNP K may induce a specific immune response to hnRNP K in patients with immune-mediated AA.

The ELISA detected significantly higher titers of anti-hnRNP K Abs in comparison to healthy controls in 56 (36%) of 155 patients with immune-mediated AA displaying increased PNH-type cells and in 29 (25%) of 118 patients without increased PNH-type cells in the current study, and there was no significant difference in the prevalence of anti-hnRNP K Abs between these two groups. High titers of anti-hnRNP K Abs were also detected in 24% of RA patients not showing apparent signs of pancytopenia. Similarly, a previous study demonstrated the presence of anti-hnRNP K Abs in 14% of RA patients [33]. Therefore, anti-hnRNP K Ab is not considered to be a specific marker for the presence of the immune attack against hematologic stem cells. However, a case–control study on AA conducted by the International Agranulocytosis and AA Study revealed that a past history of RA is significantly associated with the subsequent development of AA [34], and previous studies revealed the presence of anti-

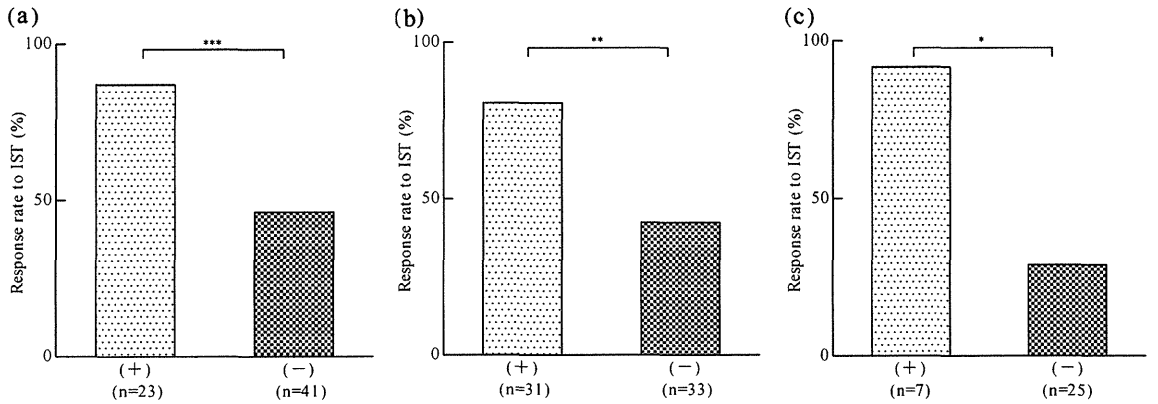

Fig. 4 The relationships between anti-hnRNP K Abs and response rate to IST in patients with BMF. The response rates to IST were compared between the following patient groups. **a** Patients with anti-hnRNP K Abs (+) and those without anti-hnRNP K Abs (−). **b** Patients showing at least one Ab^+ of three auto-Abs (+) and patients not showing Ab^+ in any of the three auto-Abs (−). **c** PNH^- patients with anti-hnRNP K Ab^+ (+) and those anti-hnRNP K Ab^- (−) (***P= 0.0015, **P=0.0022, *P=0.0265)

moesin Abs in 14% of patients with RA and in 37% of patients with AA [13, 35]. These findings suggest that AA and RA may share pathogenetic mechanisms characterized by a breakdown of immune tolerance to moesin and hnRNP K. It remains unclear why bone marrow failure develops only in AA despite the sharing of immune mechanisms. Although a breakdown of immune tolerance toward multiple autoantigens occurs in both diseases, the breakdown toward antigens on hematopoietic stem cells may occur only in patients with AA.

A strong correlation was found between the presence of anti-hnRNP K Abs and that of anti-DRS-1 Abs or anti-moesin Abs in patients with AA in the present study, indicating that a propensity of patients with immune-mediated AA thus undergo a breakdown of immune tolerance toward multiple autoantigens, possibly including pathogenic autoantigens in AA. Therefore, anti-hnRNP K Abs may serve as an indirect marker for the presence of immune pathophysiology of AA. Indeed, the presence of anti-hnRNP K Abs predicted a response to IST either by itself or in combination with anti-DRS-1 Abs or anti-moesin Abs, even in PNH^- patients with AA (Fig. 4). Among the three different Abs, only the presence of anti-hnRNP K Abs proved to be a significant factor for a good response to IST based on a multivariate analysis. Therefore, the detection of anti-hnRNP K Abs alone or together with anti-DRS-1 Abs and anti-moesin Abs may be useful in choosing the optimal therapy for AA patients, particularly when PNH-type cell detection is inapplicable. Recent reports showed that some patients with AA improved with anti-CD20 Ab (rituximab) therapy [36, 37]. The detection of these auto-Abs may also be useful for identifying AA patients who are likely to respond to such anti-CD20 Ab therapy.

Fritsch et al. [38] recently reported that hnRNP A2-specific T cell clones from patients with RA show a strong Th1 phenotype and secrete higher amounts of IFN-γ than Th1 clones from controls. Inhibition experiments performed with mAb specific to MHC class II molecules show that the hnRNP A2-induced T cell responses are largely HLA-DR restricted. $CD4^+$ T cells play an important role in the development of AA as well as of HLA-DRB1*1501 [9, 12]. Specific immune responses to hnRNP K may induce the polarization of Th1 $CD4^+$ cells and may thereby contribute to development of AA. Identification of hnRNP K-specific T cells with HLA class II tetramers and a functional analysis of those would help further clarify the roles of immune response specific to hnRNP K in the pathophysiology of AA.

Table 2 Pretreatment variables associated with a response to ATG plus CsA therapy

Favorable factors	*P* value	
	Univariate[a]	Multivariate[b]
Gender (male vs. female)	1.0000	0.8770
Age (at least 40 years vs. younger)	1.0000	0.4380
Severity (severe vs. moderate)	0.5085	0.8540
PNH-type cell (positive vs. negative)	0.0097	0.0370
Anti-DRS-1 Abs (positive vs. negative)	0.5610	0.7800
Anti-moesin Abs (positive vs. negative)	0.0036	0.5800
Anti-hnRNP K Abs (positive vs. negative)	0.0004	0.0120

[a] Fisher's exact probability test

[b] Wald c^2 test for a logistic regression model

Acknowledgments The authors would like to thank R. Oumi and T. Tanaka of Cellular Transplantation Biology of Kanazawa University who provided some technical assistance and all of the BMF study groups who provided sera of patients to this study. This work was supported by a grant from Grant-in-Aid for Scientific Research from the Ministry of Education, Science, Technology, Sports and Culture of Japan (KAKENHI No. 21390291) and grants from the Research Committee for Idiopathic Hematopoietic Disorders, the Ministry of Health, Labor, and Welfare, Japan.

References

1. Rosenfeld SJ, Kimball J, Vining D, Young NS (1995) Intensive immunosuppression with antithymocyte globulin and cyclosporine as treatment for severe acquired aplastic anemia. Blood 85 (11):3058–3065
2. Bacigalupo A, Broccia G, Corda G, Arcese W, Carotenuto M, Gallamini A, Locatelli F, Mori PG, Saracco P, Todeschini G, Coser P, Iacopino P, Vanlint MT, Gluckman E (1995) Antilymphocyte globulin, cyclosporin, and granulocyte colony-stimulating factor in patients with acquired severe aplastic anemia (SAA): a pilot study of the EBMT SAA Working Party. Blood 85(5):1348–1353
3. Maciejewski JP, Hibbs JR, Anderson S, Katevas P, Young NS (1994) Bone marrow and peripheral blood lymphocyte phenotype in patients with bone marrow failure. Exp Hematol 22(11):1102–1110
4. Nakao S, Yamaguchi M, Shiobara S, Yokoi T, Miyawaki T, Taniguchi T, Matsuda T (1992) Interferon-gamma gene expression in unstimulated bone marrow mononuclear cells predicts a good response to cyclosporine therapy in aplastic anemia. Blood 79 (10):2532–2535
5. Sloand E, Kim S, Maciejewski JP, Tisdale J, Follmann D, Young NS (2002) Intracellular interferon-gamma in circulating and marrow T cells detected by flow cytometry and the response to immunosuppressive therapy in patients with aplastic anemia. Blood 100(4):1185–1191
6. Takami A, Nakao S, Tatsumi Y, Wang HB, Zeng WH, Yamazaki H, Yasue S, Shiobara S, Matsuda T, Mizoguchi H (1999) High inducibility of heat shock protein 72 (hsp72) in peripheral blood mononuclear cells of aplastic anaemia patients: a reliable marker of immune-mediated aplastic anaemia responsive to cyclosporine therapy. Br J Haematol 106(2):377–384
7. Nakao S, Takamatsu H, Chuhjo T, Ueda M, Shiobara S, Matsuda T, Kaneshige T, Mizoguchi H (1994) Identification of a specific HLA class II haplotype strongly associated with susceptibility to cyclosporine-dependent aplastic anemia. Blood 84(12):4257–4261
8. Sugimori C, Chuhjo T, Feng XM, Yamazaki H, Takami A, Teramura M, Mizoguchi H, Omine M, Nakao S (2006) Minor population of CD55(-)CD59(-) blood cells predicts response to immunosuppressive therapy and prognosis in patients with aplastic anemia. Blood 107(4):1308–1314. doi:10.1182/blood-2005-06-2485
9. Sugimori C, Yamazaki H, Feng XM, Mochizuki K, Kondo Y, Takami A, Chuhjo T, Kimura A, Teramura M, Mizoguchi H, Omine M, Nakao S (2007) Roles of DRB1*1501 and DRB1*1502 in the pathogenesis of aplastic anemia. Exp Hematol 35(1):13–20. doi:10.1016/j.exphem.2006.09.002
10. Berger T, Rubner P, Schautzer F, Egg R, Ulmer H, Mayringer I, Dilitz E, Deisenhammer F, Reindl M (2003) Antimyelin antibodies as a predictor of clinically definite multiple sclerosis after a first demyelinating event. N Engl J Med 349(2):139–145
11. Ronkainen MS, Harkonen T, Perheentupa J, Knip M (2005) Characterization of the humoral immune response to glutamic acid decarboxylase in patients with autoimmune polyendocrinopathy-candidiasis-ectodermal dystrophy (APECED) and/or type 1 diabetes. Eur J Endocrinol 153(6):901–906. doi:10.1530/eje.1.02026
12. Feng XM, Chuhjo T, Sugimori C, Kotani T, Lu XZ, Takami A, Takamatsu H, Yamazaki H, Nakao S (2004) Diazepam-binding inhibitor-related protein 1: a candidate autoantigen in acquired aplastic anemia patients harboring a minor population of paroxysmal nocturnal hemoglobinuria-type cells. Blood 104(8):2425–2431. doi:10.1182/blood-2004-05-1839
13. Takamatsu H, Feng XM, Chuhjo T, Lu XZ, Sugimori C, Okawa K, Yamamoto M, Iseki S, Nakao S (2007) Specific antibodies to moesin, a membrane-cytoskeleton linker protein, are frequently detected in patients with acquired aplastic anemia. Blood 109 (6):2514–2520. doi:10.1182/blood-2006-07-036715
14. Nyman TA, Rosengren A, Syyrakki S, Pellinen TP, Rautajoki K, Lahesmaa R (2001) A proteome database of human primary T helper cells. Electrophoresis 22(20):4375–4382
15. Jensen ON, Podtelejnikov A, Mann M (1996) Delayed extraction improves specificity in database searches by matrix-assisted laser desorption/ionization peptide maps. Rapid Commun Mass Spectrom 10(11):1371–1378
16. Yates JR (1998) Mass spectrometry and the age of the proteome. J Mass Spectrom 33(1):1–19
17. Camitta BM (2000) What is the definition of cure for aplastic anemia? Acta Haematol 103(1):16–18
18. Caporali R, Bugatti S, Bruschi E, Cavagna L, Montecucco C (2005) Autoantibodies to heterogeneous nuclear ribonucleoproteins. Autoimmunity 38(1):25–32. doi:10.1080/08916930400022590
19. Hassfeld W, Steiner G, Hartmuth K, Kolarz G, Scherak O, Graninger W, Thumb N, Smolen JS (1989) Demonstration of a new antinuclear antibody (anti-RA33) that is highly specific for rheumatoid arthritis. Arthritis Rheum 32(12):1515–1520
20. GA DA, Vretou E, Sekeris CE (1988) Autoantibodies to the core proteins of hnRNPs. FEBS Lett 231(1):118–124
21. KE JL, Wilson SH, Steinberg AD, Klinman DM (1988) Antibodies from patients and mice with autoimmune diseases react with recombinant hnRNP core protein A1. J Autoimmun 1(1):73–83
22. Montecucco C, Caporali R, Negri C, de Gennaro F, Cerino A, Bestagno M, Cobianchi F, Astaldi-Ricotti GC (1990) Antibodies from patients with rheumatoid arthritis and systemic lupus erythematosus recognize different epitopes of a single heterogeneous nuclear RNP core protein. Possible role of cross-reacting antikeratin antibodies. Arthritis Rheum 33(2):180–186
23. Steiner G, Hartmuth K, Skriner K, Maurerfogy I, Sinski A, Thalmann E, Hassfeld W, Barta A, Smolen JS (1992) Purification and partial sequencing of the nuclear autoantigen RA33 shows that it is indistinguishable from the A2 protein of the heterogeneous nuclear ribonucleoprotein complex. J Clin Investig 90(3):1061–1066
24. Hassfeld W, Steiner G, Studnickabenke A, Skriner K, Graninger W, Fischer I, Smolen JS (1995) Autoimmune response to the spliceosome. An immunologic link between rheumatoid arthritis, mixed connective tissue disease, and systemic lupus erythematosus. Arthritis Rheum 38(6):777–785
25. Jones DA, Yawalkar N, Suh KY, Sadat S, Rich B, Kupper TS (2004) Identification of autoantigens in psoriatic plaques using expression cloning. J Investig Dermatol 123(1):93–100. doi:10.1111/j.0022-202X.2004.22709.x
26. Bomsztyk K, VanSeuningen I, Suzuki H, Denisenko O, Ostrowski J (1997) Diverse molecular interactions of the hnRNP K protein. FEBS Lett 403(2):113–115
27. Bomsztyk K, Denisenko O, Ostrowski J (2004) HnRNP K: One protein multiple processes. Bioessays 26(6):629–638. doi:10.1002/bies.20048
28. Mandal M, Vadlamudi R, Nguyen D, Wang RA, Costa L, Bagheri-Yarmand R, Mendelsohn J, Kumar R (2001) Growth factors regulate heterogeneous nuclear ribonucleoprotein K expression and function. J Biol Chem 276(13):9699–9704

29. Li C, Hong Y, Tan YX, Zhou H, Ai JH, Li SJ, Zhang L, Xia QC, Wu JR, Wang HY, Zeng R (2004) Accurate qualitative and quantitative proteomic analysis of clinical hepatocellular carcinoma using laser capture microdissection coupled with isotope-coded affinity tag and two-dimensional liquid chromatography mass spectrometry. Mol Cell Proteomics 3(4):399–409. doi:10.1074/mcp.M300133-MCP200
30. Hatakeyama H, Kondo T, Fujii K, Nakanishi Y, Kato H, Fukuda S, Hirohashi S (2006) Protein clusters associated with carcinogenesis, histological differentiation and nodal metastasis in esophageal cancer. Proteomics 6(23):6300–6316. doi:10.1002/pmic.200600488
31. Klimek-Tomczak K, Mikula M, Dzwonek A, Paziewska A, Karczmarski J, Hennig E, Bujnicki JM, Bragoszewski P, Denisenko O, Bomsztyk K, Ostrowski J (2006) Editing of hnRNP K protein mRNA in colorectal adenocarcinoma and surrounding mucosa. Br J Cancer 94(4):586–592. doi:10.1038/sj.bjc.6602938
32. Notari M, Neviani P, Santhanam R, Blaser BW, Chang JS, Galietta A, Willis AE, Roy DC, Caligiuri MA, Marcucci G, Perrotti D (2006) A MAPK/HNRPK pathway controls BCR/ABL oncogenic potential by regulating MYC mRNA translation. Blood 107(6):2507–2516. doi:10.1182/blood-2005.09.3732
33. Valai A, Belisova A, Hayer S, Hoefler E, Steiner G (2004) The RNA binding domains of hnRNP K contain major autoepitopes targeted by patients with SLE and other autoimmune diseases. In: ICI/FOCISed. Abstract number 1148
34. Kaufman DW, Kelly JP, Levy M, Shapiro S (eds) (1991) The drug etiology of agranulocytosis and aplastic anemia: the international agranulocytosis and aplastic anemia study. Oxford University Press, New York
35. Wagatsuma M, Kimura M, Suzuki R, Takeuchi F, Matsuta K, Watanabe H (1996) Ezrin, radixin and moesin are possible autoimmune antigens in rheumatoid arthritis. Mol Immunol 33 (15):1171–1176
36. Hansen PB, Lauritzen AMF (2005) Aplastic anemia successfully treated with rituximab. Am J Hematol 80(4):292–294. doi:10.1002/ajh.20428
37. Castiglioni MG, Scatena P, Pandolfo C, Mechelli S, Bianchi M (2006) Rituximab therapy of severe aplastic anemia induced by fludarabine and cyclophosphamide in a patient affected by B-cell chronic lymphocytic leukemia. Leuk Lymphoma 47(9):1985–1986. doi:10.1080/10428190600709630
38. Fritsch R, Eselbock D, Skriner K, Jahn-Schmid B, Scheinecker C, Bohle B, Tohidast-Akrad M, Hayer S, Neumuller J, Pinol-Roma S, Smolen JS, Steiner G (2002) Characterization of autoreactive T cells to the autoantigens heterogeneous nuclear ribonucleoprotein A2 (RA33) and filaggrin in patients with rheumatoid arthritis. J Immunol 169(2):1068–1076

European Journal of Haematology 86 (226–236)

ORIGINAL ARTICLE

GPI-anchored protein-deficient T cells in patients with aplastic anemia and low-risk myelodysplastic syndrome: implications for the immunopathophysiology of bone marrow failure

Takamasa Katagiri[1,2], Zhirong Qi[2], Shigeki Ohtake[1], Shinji Nakao[2]

[1]Clinical Laboratory Science, Division of Health Sciences; [2]Cellular Transplantation Biology, Division of Cancer Medicine, Kanazawa University Graduate School of Medical Science, Kanazawa, Ishikawa, Japan

Abstract

Glycosylphosphatidylinositol-anchored protein-deficient (GPI-AP$^-$) T cells can be detected in some patients with bone marrow failure (BMF), but the link between these cells and BMF pathophysiology remains to be elucidated. To clarify the significance of GPI-AP$^-$ T cells in BMF, peripheral blood from 562 patients was examined for the presence of CD48$^-$CD59$^-$CD3$^+$ cells using high-resolution flow cytometry (FCM), and the GPI-AP$^-$ T cells were characterized with regard to their phenotype and sensitivity to inhibitory molecules, including herpesvirus entry mediator (HVEM) and a myelosuppressive cytokine, TGF-β. A multi-lineage FCM analysis detected CD48$^-$CD59$^-$CD3$^+$ T cells in 72 (12.8%) of the patients, together with GPI-AP$^-$ myeloid cells. Unexpectedly, 12 patients (10 with aplastic anemia and 2 with myelodysplastic syndrome-refractory anemia, 2.1%), who showed clinical features similar to those of other BMF patients with GPI-AP$^-$ myeloid cells, such as a good response to immunosuppressive therapy, displayed 0.01–0.3% GPI-AP$^-$ cells exclusively in T cells. The CD48$^-$CD59$^-$ T cells consisted of predominantly effector memory (EM) and terminal effector cells, while CD48$^-$CD59$^-$ T cells from non-BMF patients who had received anti-CD52 antibody only showed EM and central memory phenotypes. TGF-β and HVEM capable of inhibiting T-cell proliferation via its GPI-AP CD160 ligation suppressed the *in vitro* proliferation of GPI-AP$^+$ T cells more potently than that of GPI-AP$^-$ T cells from the same patients. The presence of GPI-AP$^-$ T cells, as well as GPI-AP$^-$ myeloid cells, may therefore reflect the immunopathophysiology of BMF in which cytokine-mediated suppression of hematopoietic stem cells via GPI-AP-type receptors takes place.

Key words aplastic anemia; myelodysplastic syndrome; paroxysmal nocturnal hemoglobinuria; GPI-anchored protein-deficient T cells

Correspondence Shinji Nakao, Cellular Transplantation Biology, Division of Cancer Medicine, Kanazawa University Graduate School of Medical Science, 13-1 Takaramachi Kanazawa, Ishikawa, Japan. Tel: +81 762 652 274; Fax: +81 762 34 4252; e-mail:snakao@med3.m.kanazawa-u.ac.jp

Accepted for publication 16 December 2010

doi:10.1111/j.1600-0609.2010.01563.x

Small populations of glycosylphosphatidylinositol-anchored protein-deficient (GPI-AP$^-$) blood cells are often detectable in the peripheral blood (PB) of patients with aplastic anemia (AA) and low-risk myelodysplastic syndrome (MDS) such as refractory anemia (RA) and refractory cytopenia with multilineage dysplasia (1–6). Although such GPI-AP$^-$ blood cells often comprise $<1\%$ of granulocytes or erythrocytes, they are thought to be derived from hematopoietic stem cells (HSCs) with a *PIGA* mutation rather than committed progenitor cells because GPI-AP$^-$ granulocytes persists for many years, maintaining their individual scattergram profiles (7). Several studies have identified the presence of small populations of GPI-AP$^-$ cells as a significant factor predicting a good response to immunosuppressive therapy (IST) in patients with AA and low-risk MDS (4–6, 8–10).

Immune mechanisms are therefore thought to be involved in the increase in the GPI-AP$^-$ cells in such bone marrow failure (BMF), though the exact mechanisms responsible for the increase in the GPI-AP$^-$ cells remain unknown.

The most widely accepted mechanism for clonal expansion of GPI-AP$^-$ cells in patients with BMF is the 'escape hypothesis', which states that the relative number of *PIGA* mutant HSCs increases by avoiding immunologic attacks by T cells or NK cells (11–17). Consistent with the escape hypothesis, GPI-AP deficient cells are usually detectable in many lineages of cells, including monocytes, lymphocytes and NK cells, in addition to granulocytes and erythrocytes, in patients with classical paroxysmal nocturnal hemoglobinuria (PNH) (18–21). However, the screening of multi-lineage PB cells from patients with BMF for the presence of GPI-AP$^-$ cells using high-sensitivity flow cytometry unexpectedly revealed a few patients who showed GPI-AP$^-$ cells only in T cells (unpublished observation). The presence of GPI-AP$^-$ T cells alone appeared to contradict the escape mechanism because T-cell precursors are not the target of immune system attack in BMF. Therefore, the multi-lineage analysis was extended to a larger number of patients to determine the significance of GPI-AP$^-$ T cells in patients with BMF. The phenotypic and functional analyses of such GPI-AP$^-$ T cells provided evidence that, just like GPI-AP$^-$ myeloid cells, GPI-AP$^-$ T cells reflect the immunopathophysiology of BMF, in which the cytokine-mediated suppression of HSCs via GPI-AP-type receptors takes place.

Patients and methods

Patients and healthy volunteers

The PBs of 562 patients with various types of cytopenias were examined for the presence of GPI-AP$^-$ cells using high-sensitivity flow cytometry. Their diagnoses included classic PNH in 13, AA in 348, and MDS-RA in 201. The subgroups of MDS were defined according to the FAB classification (22). The male-to-female ratio was 1 : 1.2 (255 : 307), and the median age was 56 yr (range: 1–95 yr). PB samples from three patients (one with acute myelogenous leukemia and two with AA) who were conditioned with alemtuzumab (Campath1-H), a humanized monoclonal antibody (mAb) specific to CD52, for allogeneic stem cell transplantation as well as from 57 healthy individuals were also examined for the presence of GPI-AP$^-$ cells in all lineages of cells. All patients and healthy individuals provided their informed consent before sampling. This study protocol was approved by the ethics committee of Kanazawa University Graduate School of Medical Science.

Monoclonal antibodies (mAbs)

mAbs used for multicolor flow cytometry were anti-CD59 labeled with FITC (P282E, IgG2a; Beckman Coulter, Miami, FL, USA), anti-CD59 labeled with PE (H19, IgG2a; BD Pharmingen, San Diego, CA, USA), anti-CD55 labeled with FITC (IA10, IgG2a; BD Pharmingen), anti-CD48 labeled with FITC (J4-57, IgG1; Beckman Coulter), anti-CD48 labeled with PE (156-4H9, IgG1; eBioscience, San Diego, CA, USA), anti-CD33 labeled with APC (D3HL60.251, IgG1; Beckman Coulter), anti-CD19 labeled with APC-Cy7 (SJ25C1, IgG1; BD Pharmingen), anti-CD335 labeled with PE (BAB281, IgG1; Beckman Coulter), anti-CD3 labeled with PerCP-Cy5.5 (SK7, IgG1; BD Pharmingen), anti-CD3 labeled with APC (UCHT1, IgG1; Beckman Coulter), anti-CD11b/Mac-1 labeled with PE (ICRF44, IgG1; BD Pharmingen), anti-glycophorin A labeled with PE (JC159, IgG1; Dako, Carpenteria, CA, USA). Phenotypic analysis of GPI-AP-deficient CD3$^+$ T lymphocyte was carried out by additional staining with mAbs specific to CD45RA labeled with PE (HI100, IgG2b; BD Pharmingen), CD62L labeled with APC (DREG-56, IgG1; BD Pharmingen), CD197 labeled with PE-Cy7 (3D12, IgG2a; BD Pharmingen), CD4 labeled with APC-Cy7 (RPA-T4, IgG1; BD Pharmingen), CD8 labeled with APC-Cy7 (SK1, IgG1; BD Pharmingen).

Flow cytometry for detecting GPI-AP$^-$ cells and determining GPI-AP$^-$ T-cell phenotype

Six lineages of blood cells including granulocytes, erythrocytes, monocytes, T cells, B cells and NK cells were subjected to high-sensitivity flow cytometry for detecting small populations of GPI-AP$^-$ cells. All blood samples were analysed within 24 h to avoid false-positive results because of cell damages. The staining with the each mAb in this study was performed according to the well-established lyse-stain protocol, previously described in detail (6, 23). Briefly, 3–5 mL of heparinized blood was drawn from the patients and healthy individuals. Erythrocytes were lysed in the lysis buffer containing NH_4Cl 8.26 g/L, $KHCO_3$ 1.0 g/L, and EDTA · E4Na· 0.037 g/L to detect GPI-AP$^-$ leukocytes. After washing with saline, 50 μL of the leukocyte suspension was incubated with FITC-labeled anti-CD55 and anti-CD59 mAbs for granulocytes or FITC-labeled anti-CD48 and anti-CD59 mAbs for monocytes, T cells, B cells and NK cells in combination with mAbs specific for lineage markers including PE-labeled CD11b for granulocytes, APC-labeled CD33 for monocytes, PerCP-Cy5.5-labeled CD3 for T cells, APC-Cy7-labeled CD19 for B cells and PE-labeled CD335 for NK cells. Fresh

blood was diluted to 3% in phosphate-buffered saline (PBS), and then 50 μL was incubated with PE-labeled anti-glycophorin A and FITC-labeled anti-CD55 and anti-CD59 mAbs on ice for 30 min to detect GPI-AP$^-$ erythrocytes. Three-step gating excluded the debris and immature granulocytes that are frequently found in samples from patients with MDS. Step 1 involved the gating of granulocyte, lymphocyte or monocyte populations from the FSC–SSC scattergrams (R1). Step 2 involved the gating of the lineage marker^{bright} population on the lineage marker-SSC scattergram to exclude the lineage marker^{dim} cells that are features of either damaged cells or immature cells. Step 3 was the gating of R1 × R2 and the analysis of 10^6 cells on R1 × R2 scattergrams. The presence of ≥0.005% CD55$^-$CD59$^-$GP-A$^+$ erythrocytes, ≥0.003% CD55$^-$CD59$^-$CD11b$^+$ granulocytes, and ≥0.01% CD55$^-$CD59$^-$ CD33$^+$ monocytes, CD48$^-$CD59$^-$ CD3$^+$ T cells, CD48$^-$CD59$^-$CD19$^+$ B cells and CD48$^-$CD59$^-$ CD335$^+$ NK cells was defined as an abnormal increase (positive) based on the results obtained from 57 healthy individuals (6). When GPI-AP$^-$ cells were detected in only one lineage of cells or the percentages of GPI-AP$^-$ cells were <0.01%, then additional samples were tested, and the patients were judged to be PNH$^+$ when the examination results of the first and second samples were identical.

The phenotype of GPI-AP-deficient-CD3$^+$ T lymphocyte was determined using anti-CD45RA, anti-CD62L and anti-CCR7 mAbs and the percentages of four different T-cell subsets including naïve (CD45RA$^+$CD62L$^+$CCR7$^+$), central memory (CM) (CD45RA$^-$CD62L$^+$CCR7$^+$), effector memory (EM) (CD45RA$^-$CD62L$^-$CCR7$^-$), and terminal effector memory (TEM) (CD45RA$^+$CD62L$^-$ CCR7$^-$) cells were determined according to the methods defined by previous reports (24, 25).

Data acquisition was performed immediately after sampling using FACSCanto II, and the data were analysed using the FACSDiva software program and percentage of each population was calculated by FlowJo software 7.6.1 (Treestar, Ashland, OR, USA).

T cell culture

PB mononuclear cells (PBMCs) were isolated using density gradient centrifugation on Ficoll/Hypaque (Fresenius Kabi Norge AS, Halden, Norway). A sample of 1×10^6 PBMCs were cultured in RPMI1640 containing 10 μg/mL phytohemagglutinin (Sigma, St. Louis, MO), 10% fetal bovine serum (FBS), 50 U/mL penicillin, 50 μg/mL streptomycin and 100 IU/mL IL-2 for 7 d. After washing with RPMI1640, the cultured cells were subjected to cell sorting in order to analyse the *PIGA* gene as described in the following paragraphs.

Cell sorting and *PIGA* gene analysis

CD48$^-$CD59$^-$CD3$^+$ freshly isolated or cultured T cells were separated from CD3$^+$ T cells with a cell sorter (JSAN; Bay Bioscience, Kobe, Japan). More than 95% of the sorted cells were GPI-AP deficient. An analysis of the *PIGA* gene mutation was performed as described previously (26). Briefly, the coding regions of *PIGA* were amplified by nested or semi-nested PCR using 12 primer sets, and six ligation reactions were used to transform competent *Escherichia coli* JM109 cells (Nippon Gene, Tokyo, Japan). Five clones were selected randomly from each group of transfectants and subjected to sequencing with BigDye Terminator v3.1 Cycle Sequencing kit (Applied Biosystems, San Diego, CA, USA) and an ABI PRISM 3100 Genetic Analyzer (Applied Biosystems).

Preparation of CD3$^+$ T cells and mAb-coated latex beads

CD3$^+$ T cells were purified from freshly isolated PBMCs by depleting non-CD3$^+$ T cells with magnetic beads using Pan T cell isolation II kit II (Miltenyi, Bergisch Gladbach, Germany); purity was judged to be over 95% by flow cytometry. Latex beads (Miltenyi) were coated with various concentration of anti-CD3 (OKT3; Miltenyi) and anti-CD28 mAbs (15E8; Miltenyi), or various concentrations of human herpesvirus entry mediator (HVEM)-Ig (mIgG1 Fc; 100-330; R&D Systems, Minneapolis, MN, USA) or mouse IgG1 (27). The mixture of latex beads were suspended in PBS and incubated for 2 h at 37°C in humid air containing 5% CO_2. The latex beads were washed once with RPMI1640 medium containing 10% FBS for 30 min at 37°C. The beads were then washed three times with PBS and thereafter were used for T-cell stimulation.

Carboxyfluorescein diacetate succinimidyl diester (CFSE) assay

CD3$^+$ T cells were washed twice with PBS and were suspended in PBS at the concentration of 5×10^6 cells/mL. One milliliter of the cell suspension was mixed with an equal volume of PBS containing 1 μM CFSE (Invitrogen, Carlsbad, CA, USA), and incubated for 10 min in a humidified atmosphere containing 5% CO_2 at 37°C with occasional mixing. Labeling was quenched by the additional of an equal volume of cold FBS, and incubated for 5 min on ice. The cells were then centrifuged and washed three times in PBS containing 1% bovine serum albumin followed by two washes with RPMI1640 containing 5% autologous serum. The cells were plated at a density of 1×10^6 cells/mL in 96-well U-bottomed plates and were incubated in the presence of anti-CD3 mAb-coated and anti-CD28 mAb-coated beads with or

without HVEM fusion protein or TGF-β (Peprotech, Rocky Hill, NJ, USA) at various concentrations. The CFSE levels in the cultured T cells were then determined 10 d later by flow cytometry. The inhibitory effects of HVEM or TGF-β on the T-cell proliferation was assessed by comparing the mean percentage of cells that underwent cell division in the presence of the inhibitory molecules with that of the control culture.

Statistical analysis

The differences in the inhibition of the decline in the CFSE level by HVEM or TGF-β between GPI-AP$^+$ and GPI-AP$^-$ T cells of individual patients were assessed by the Student's *t*-test.

Results

GPI-AP$^-$ T cells in patients with BMF

Significant populations of GPI-AP$^-$ cells were detectable in at least one lineage of cells from 252 (44.8%) of 562 patients with BMF and CD48$^-$CD59$^-$CD3$^+$ T cells were detected in 72 (12.8%) of the patients. Clone sizes of GPI-AP$^-$ cells in different lineages of cells in patients with increased GPI-AP$^-$ cells are summarized in Table 1. The GPI-AP$^-$ cells were also detected in two or more lineages of cells including granulocytes or monocytes in 60 of the GPI-AP$^-$ T cell$^+$ patients (Fig. 1A–C). However, the remaining 12 (2.1%) patients showed GPI-AP$^-$ cells only in T cells (Fig. 1D). The similar percentages (0.01–0.3%) of GPI-AP$^-$ T cells were detectable in different samples obtained from the patients at intervals of 2–6 months (Fig. 2). Such GPI-AP$^-$ T cells >0.01% were undetectable in any of 57 healthy individuals and the other 490 patients with BMF. The clinical characteristics of the 12 patients who were provisionally referred to as 'PNH-T$^+$ patients' are summarized in Table 2. All these patients had predominant thrombocytopenia without any increase in the number of BM megakaryocytes, a common feature of BMF patients possessing small populations of GPI-AP$^-$ cells (7). Five patients (patients 1, 2, 3, 9, and 11) were red blood cell or platelet transfusion-dependent, and only patient 11 had been treated with IST (ATG) before the detection of GPI-AP$^-$ T cells. Three of the PNH-T$^+$ patients received IST (ATG + cyclosporine for patients 2 and 9, and cyclosporine alone for patient 12) after the GPI-AP$^-$ cell screening. All achieved a partial remission according to the response criteria described by Camitta (28) as described previously.

Phenotype of GPI-AP$^-$ T cells detected in patients with BMF

The functional phenotypes of GPI-AP$^-$ T cells in nine PNH-T$^+$ patients, defined by the expression of CD45RA, CD62L, and CCR7 were compared to those of GPI-AP$^-$ T cells detectable in three BM transplant recipients who were conditioned with alemtuzumab (group 1) or to those detectable in 12 patients who displayed GPI-AP$^-$ cells in all lineages of blood cells including GPI-AP$^-$ T cells that account for 0.02–41.2% of total T cells (group 2). As shown in Fig. 3A, the GPI-AP$^-$ T cells in three patients from group 1 predominantly showed EM (CD45RA$^-$CD62L$^-$CCR7$^-$, EM) and CM (CD45RA$^-$CD62L$^+$CCR7$^+$, CM) phenotypes. No naïve (CD45RA$^+$CD62L$^+$CCR7$^+$) T-cell subset was observed in this group. On the other hand, the T cells from group 2 patients mainly contained cells with the naïve phenotype with relatively small percentages of CM, EM, and TEM subsets (Fig. 3B). GPI-AP$^-$ T cells in PNH-T$^+$ (group 3) patients predominantly showed the EM phenotype with smaller percentages of naïve, CM, and TEM phenotypes (Fig. 3C), suggesting the phenotypic pattern of GPI-AP$^-$ T cells in group 3 patients to be more similar to that in group 2 patients than that in non-BMF patients treated with alemtuzumab.

Table 1 Clone size of GPI-AP$^-$ cells in different lineages of cells in patients with increased GPI-AP$^-$ cells

	PNH	AA		MDS-RA	
	Median % of GPI-AP$^-$ cells (range)	% of patients with GPI-AP$^-$ cells in all AA patients	Median % of GPI-AP$^-$ cells in AA patients with increased GPI-AP$^-$ cells (range)	% of patients with GPI-AP$^-$ cells in all RA patients	Median % of GPI-AP$^-$ cells in RA patients with increased GPI-AP$^-$ cells (range)
E	25.8 (3.8–95.6)	58.4	0.04 (0.005–48.7)	53.3	0.55 (0.005–6.4)
G	56.5 (1.2–98.1)	64.4	0.07 (0.003–37.9)	57.8	1.07 (0.003–17.4)
M	82.6 (6.1–94.2)	48.4	0.11 (0.01–82.0)	46.7	3.5 (0.01–32.2)
T	0.9 (0.01–41.2)	16.8	0.44 (0.01–6.9)	9.4	0.23 (0.01–6.6)
B	4.3 (0.8–38.0)	16.0	0.01 (0.01–13.0)	12.2	0.24 (0.01–5.1)
NK	41.7 (0.6–94.9)	15.2	0.01 (0.01–75.0)	14.4	0.55 (0.01–8.5)

E, erythrocytes; G, granulocytes; M, monocytes; T, T cells; B, B cells; NK, NK cells; PNH, paroxysmal nocturnal hemoglobinuria; AA, aplastic anemia; MDS-RA, myelodysplastic syndrome-refractory anemia; GPI-AP, glycosylphosphatidylinositol-anchored protein.

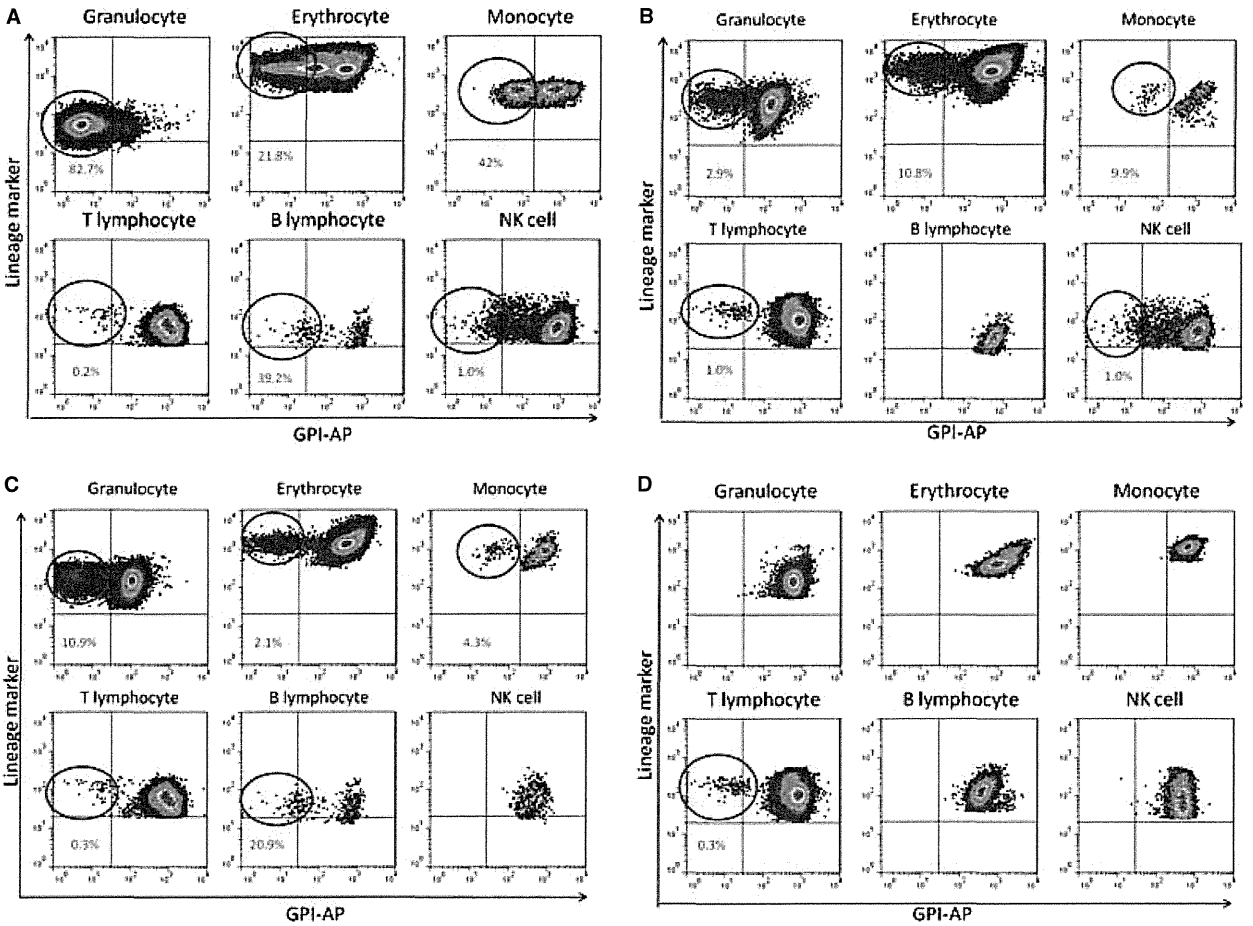

Figure 1 GPI-AP$^-$ cells in different lineages of cells. Scattergrams from four patients displaying GPI-AP$^-$ T cells are shown. (A) A patient with GPI-AP$^-$ cells in all six lineages of cells. (B) A patient with GPI-AP$^-$ cells in the granulocytes, erythrocytes, monocytes, T cells, and NK cells. (C) A patient with GPI-AP$^-$ cells in the granulocytes, erythrocytes, monocytes, T cells, and B cells. (D) A patient (patient 3) with GPI-AP$^-$ cells in T cells alone. GPI-AP, glycosylphosphatidylinositol-anchored protein.

PIGA gene analyses of GPI-AP$^-$ T cells

GPI-AP$^-$ T cells were sorted from cultured T cells from four patients (two group 1 and two group 2 patients) and were subjected to *PIGA* gene analyses. Missense mutations in exon 2 leading to a frameshift or an amino acid change were detected. These included a 16-bp deletion starting from the position of 1107 bp (frameshift), adenine insertion at the position of 1239 bp (frameshift) in group 2, the replacement of adenine (A) with guanine at 1108 bp (Arg → Gly) and 2002 bp (Gln → Arg) in a group 1 patient and the replacement of cytosine (C) with thymine (T) at 1044 bp (frameshift) and TCA insertion at 1103 bp (frameshift) in another group 1 patient.

Differences in the sensitivity to inhibitory molecules between GPI-AP$^+$ and GPI-AP$^-$ T cells

The presence of PNH-T$^+$ patients with BMF suggests that the lack of GPI-APs may confer a growth advantage to GPI-AP$^-$ T-cell precursors or memory T cells over the GPI-AP$^+$ counterparts. To test this hypothesis, T cells from three patients with BMF PNH displaying 1% and 41.2% GPI-AP$^-$ T cells were stimulated with anti-CD3 and anti-CD28 mAbs and the effects of HVEM, a ligand of a GPI-AP CD160 which inhibits T-cell proliferation upon ligation to HVEM (27), on the proliferation of GPI-AP$^-$ and GPI-AP$^+$ T cells were investigated using the CFSE assay. Figure 4 shows the results from one of the three patients which produced similar results. CD160 expression was induced on GPI-AP$^+$ T cells by anti-CD3 and anti-CD28 mAbs in a dose-dependent fashion, while the antigen was not induced on GPI-AP$^-$ T cells (Fig. 4A). Both the GPI-AP$^-$ and GPI-AP$^+$ T cells proliferated in response to anti-CD3 and anti-CD28 mAbs (Fig. 4B,C), though GPI-AP$^-$ T cells tended to show greater proliferation than GPI-AP$^+$ T cells in keeping with previous reports (29, 30). The addition of HVEM-IgG inhibited the decline in the CFSE level of GPI-AP$^+$ T cells more

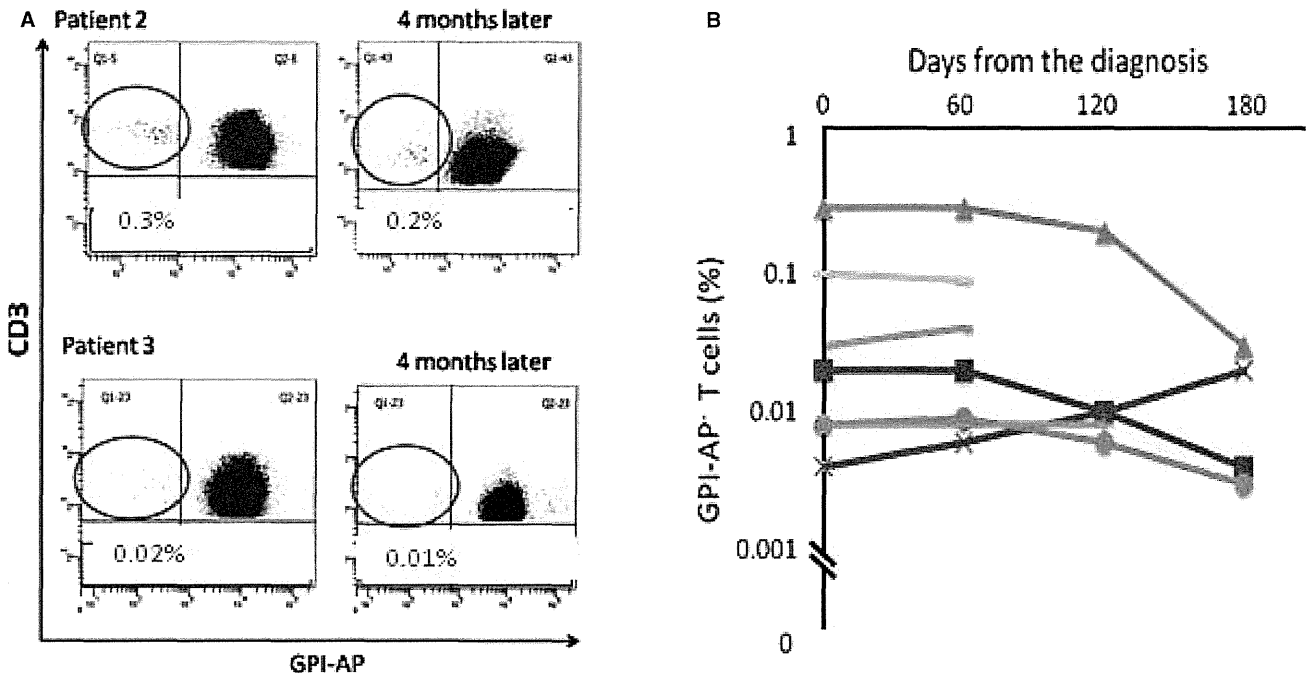

Figure 2 Changes in the percentage of GPI-AP$^-$ cells over time. (A) Scattergrams of samples obtained at 4 month internals from two PNH-T$^+$ patients are shown. (B) PB samples were obtained from the PNH-T$^+$ patients at 2-month intervals and the percentages of GPI-AP$^-$ T cells were serially determined. PNH, paroxysmal nocturnal hemoglobinuria; PB, peripheral blood; GPI-AP, glycosylphosphatidylinositol-anchored protein.

Table 2 Hematologic parameters of patients with GPI-AP$^-$ T cells alone

Patient no.	Diagnosis	Duration of illness (months)	Age at diagnosis (yr)	Gender	WBC count ($\times 10^9$/L)	Neutrophil count ($\times 10^9$/L)	Lymphocyte count ($\times 10^9$/L)	RBC count ($\times 10^{12}$/L)	Reticulocyte count ($\times 10^9$/L)	Hemoglobin (g/dL)	Platelet count ($\times 10^9$/L)	PNH-type T cell percentage
1	MAA	1	80	M	2.4	0.8	1.4	2.73	4.5	9.7	6.8	0.01
2	SAA	1	64	F	1.7	0.2	1.1	3.57	6.6	10.6	200	0.02
3	SAA	120	22	F	1.2	0.3	0.9	2.62	1.3	8.2	4	0.3
4	MAA	74	35	M	6.1	2.7	1.8	2.78	3.3	10.1	52	0.02
5	MAA	84	12	M	3.2	1	2	4.05	3.4	12.7	49	0.03
6	MDS-RA	4	59	M	5.7	2.9	2.7	2.06	5.6	10	53	0.02
7	SAA	12	61	F	1.2	0.4	0.6	2.52	0.8	7.6	12	0.01
8	MAA	108	83	F	2	1	0.8	3.51	3.2	9.8	64	0.03
9	MAA	49	26	F	2.6	0.9	1.2	2.22	4	7.3	0.8	0.1
10	MAA	120	59	M	2.1	0.8	1.2	1.56	2	5.9	0.9	0.03
11	MAA	1	76	M	2.7	1.1	1.5	4.03	4	12.4	8.2	0.3
12	MDS-RA	147	63	M	3.2	1.2	1.9	2.13	3.8	7.3	3	0.01

PNH, paroxysmal nocturnal hemoglobinuria; MDS-RA, myelodysplastic syndrome-refractory anemia; GPI-AP, glycosylphosphatidylinositol-anchored protein.

potently (27, 31, 32) than that of GPI-AP$^-$ T cells (Fig. 4B, 19.4 ± 8.1 vs. 0.7 ± 0.5 at 10 μg/mL, $P = 0.03$ and 57.5 ± 12.7 vs. 4.4 ± 4.9 at 50 μg/mL, $P = 0.004$). The GPI-AP$^-$ T-cell proliferation was not affected, even by a high concentration (50 μg/mL) of HVEM, which clearly inhibited GPI-AP$^+$ T-cell proliferation. Similarly, the addition of TGF-β tended to show a greater inhibition of the decline in the CFSE level of GPI-AP$^+$ T cells than that of GPI-AP$^-$ T cells (Fig. 4C, 17.4 ± 10.5 vs. 1.1 ± 0.5 at 5 ng/mL, $P = 0.06$ and 33.2 ± 16.2 vs. 2.1 ± 1.8 at 100 ng/mL, $P = 0.05$). These findings suggest that GPI-AP$^-$ CD3$^+$ T-cell precursors or memory T cells may preferentially proliferate *in vivo* in the presence of some ligands that transmit inhibitory signals for cell proliferation by their ligation to GPI-AP receptors.

Discussion

The present multi-lineage analysis of blood cells with high-sensitivity flow cytometry revealed CD48$^-$CD59$^-$ T

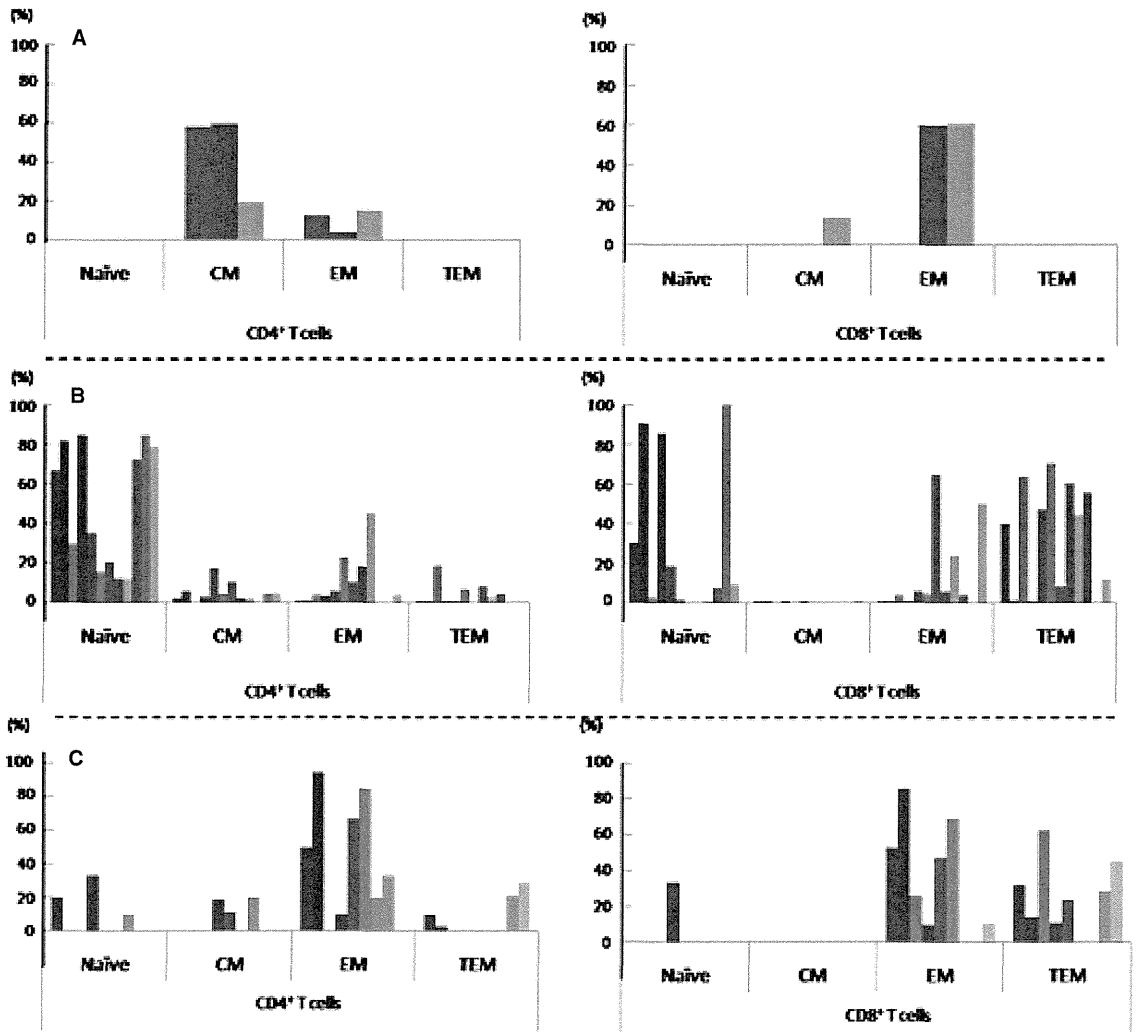

Figure 3 Phenotypic patterns of GPI-AP$^-$ T cells in different patient groups. The percentages of four different T-cell subsets defined by the expression of CD45RA, CCR7 and CD62L in CD4$^+$ and CD8$^+$ GPI-AP$^-$ T cells are shown. (A) Alemtuzumab-treated patients (n = 3); (B) bone marrow failure patients showing GPI-AP$^-$ cells in all lineages of blood cells (n = 12); (C) PNH-T$^+$ patients (n = 9). CM, central memory cells; EM, effector memory cells; TEM, terminal effector memory cells; PNH, paroxysmal nocturnal hemoglobinuria; GPI-AP, glycosylphosphatidylinositol-anchored protein.

cells in 12.8% of patients with various type of BMF. Although the percentage of GPI-AP$^-$ T cells in these patients was very low, such an increase in GPI-AP$^-$ T cells was undetectable in 57 healthy individuals and they persisted more than 2 months. The presence of GPI-AP$^-$ T cells was originally interpreted to indicate the ability of *PIGA* mutant HSC in the BMF patients to differentiate into multi-lineage blood cells (18–21). However, the GPI-AP$^-$ cells were undetectable in any other lineages of cells other than T cells in PNH-T$^+$ patients whose clinical features were similar to those of other BMF patients with GPI-AP$^-$ myeloid cells. The presence of such PNH-T$^+$ patients within the population of patients with immune-mediated BMF cannot be explained by the escape of GPI-AP$^-$ cells from T-cell attack against T-cell precursors, because T-cell precursors are not the specific target of the immune attack in patients with BMF.

The presence of PNH-T$^+$ patients can be explained by several mechanisms. One possibility is that the CD48$^-$CD59$^-$ T cells are remnants of GPI-AP$^-$ cells that used to be present in other lineages of cells. A previous study showed GPI-AP$^-$ T cells to persist in patients who underwent remission of PNH probably due to their longevity (33). The patients with long-standing disease like patients 3, 10, and 12 may have possessed small populations of GPI-AP$^-$ cells in the myeloid cells after the disease onset and lost all but the T cells with time.

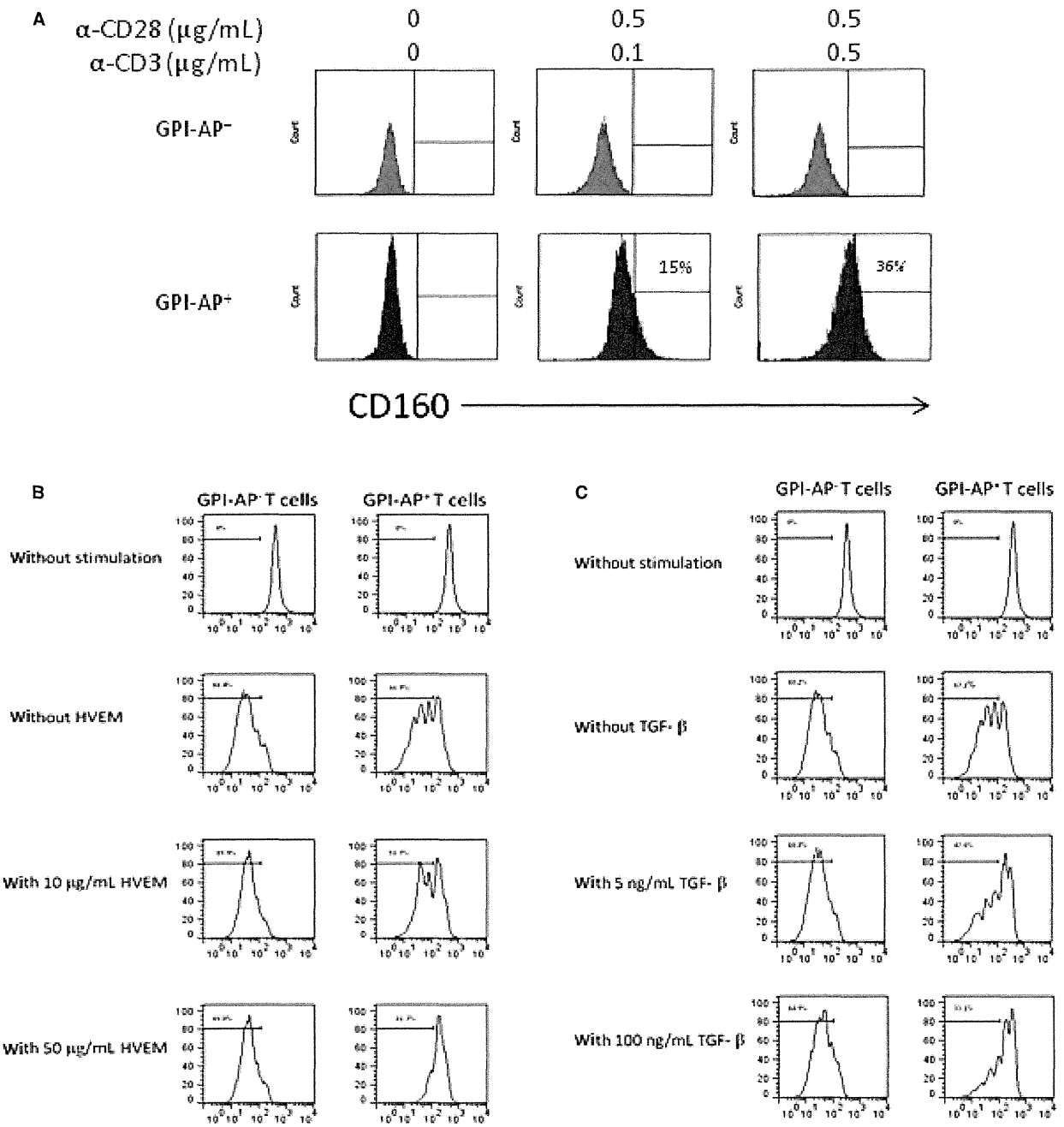

Figure 4 The effects of HVEM and TGF-β on the proliferation of GPI-AP$^+$ and GPI-AP$^-$ T cells induced by anti-CD3 and anti-CD28 mAb stimulation. PB CD3$^+$ T cells from three bone marrow failure patients were cultured in the presence of anti-CD3 and anti-CD28 mAbs for 10 d with or without HVEM and TGF-β. (A) CD160 expression by GPI-AP$^+$ T cells induced by anti-CD3 and anti-CD28 mAb stimulation compared with GPI-AP$^-$ T cells. The numbers show the percentage of CD160$^+$ cells. T-cell proliferation in the presence of different concentrations of HVEM (B) or TGF-β (C) was assessed using the carboxyfluorescein diacetate succinimidyl diester assay. The figures show representative results from one patient. The numbers denote the percentage of cells which underwent cell division. PB, peripheral blood; HVEM, herpesvirus entry mediator; GPI-AP, glycosylphosphatidylinositol-anchored protein.

However, this mechanism cannot account for PNH-T$^+$ patients in which the disease persisted for <1 yr. Another possibility is that mechanisms other than immune-mediated attack against HSCs confer proliferative advantage to GPI-AP$^-$ T-cell precursors or memory T cells. The treatment of patients with lymphoid malignancies or allogeneic stem cell transplant recipients with anti-CD52 mAb allows proliferation of GPI-AP$^-$ T cells that existed in the patients or BM donors before treatment (34, 35). Indeed, donor-derived CD48$^-$CD59$^-$